

Audun Ryland

# Simulation and Validation of a Vibrating Boring Bar

Masteroppgave i Produktutvikling og produksjon

Veileder: Knut Sørby

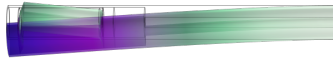
Juni 2023





Audun Ryland

# Simulation and Validation of a Vibrating Boring Bar



Masteroppgave i Produktutvikling og produksjon  
Veileder: Knut Sørby  
Juni 2023

Norges teknisk-naturvitenskapelige universitet  
Fakultet for ingeniørvitenskap  
Institutt for maskinteknikk og produksjon



Kunnskap for en bedre verden





DEPARTMENT OF  
MECHANICAL AND INDUSTRIAL ENGINEERING

TPK4940 - MANUFACTURING TECHNOLOGY, MASTER'S THESIS

---

# Simulation and Validation of a Vibrating Boring Bar

---

*Author:*  
Audun Ryland

*Advisor:*  
Knut Sørby

Date of submission: 26/06/2023

---

# 1 Abstract

## 1.1 English/Engelsk

Vibration-damped tool holders have become popular in the machining industry due to their capability to avoid vibrations, enabling longer tool life, making higher length/diameter ratios possible, and increasing the metal removal rate. A vibration-damped tool holder and simulations of it are put in the spotlight of this thesis.

Elements of a vibration-damped tool holder shall be modeled and simulated in Comsol Multiphysics. Special emphasis is put on simulating rubber and tuning the rubber material model parameters based on lab data to improve the simulation. The simulation results will be validated against real-world lab measurements.

Throughout the thesis, a high degree of independent development has been put into the simulations and an effort to gain knowledge in the field of vibrations and damping. Attending lab experiments at Sandvik Teeness gave me crucial insight, providing me with impulse response data that enabled parameter tuning and validation of the simulations.

The lab experiments and simulations were compared against each other in the frequency response curve. The simulation results are plotted by monitoring the response at a selected point of the structure when a harmonic perturbation load is acting on the system, sweeping the load over a predefined range of frequencies at discrete steps. The Lab results are monitored by a force sensor at the impact hammer and an accelerometer, processed by Sandvik and presented as frequency response with real and imaginary parts, finally computed to give the magnitude in the frequency response curve, making a relevant comparison of the simulation and lab results possible.

After tuning the rubber material parameters used in the simulations based on appropriate data from lab experiments, the results gave surprisingly good results both in terms of frequency and magnitude accuracy. The simulation's ability to predict correctly when it comes to the frequencies of the magnitude peaks from the lab data is very good, with less than 4% error. The magnitude accuracy in the frequency response was set as a secondary priority, but still performs quite well, with an average peak value error of 73%. Scaling the simulation magnitude based on the first peak value of the lab and simulation frequency response curves, reduced the average error to 60%

In light of the project goals and objectives, the thesis is seen as a personal success, creating a solid foundation for further work and development. In order to provide companies like Sandvik with useful results, there is still a lot of work to do. different roots of error must be investigated as well as running simulations with a more sophisticated simulation solver that require more computational power than what was in my reach through the thesis.

---

## 1.2 Norwegian/Norsk

Dempede dreiebomer har blitt populær i maskinerings industrien grunnet deres evne til å unngå vibrasjoner under bearbeiding. Deres egenskaper gir økt levetid på vendeskjær(kuttende del av verktøyet), muliggjør høyere lengde/diameter-forhold, og økt metallfjerningsrate. En vibrasjonsdempet dreiebom og simulering av den blir tatt under lupen i denne rapporten.

En vibrasjonsdempet dreiebom og dens komponenter skal simuleres i Comsol Multiphysics. Et økt fokus skal legges på simulering av gummi og justering av sentrale parametre i gummiens materialmodell basert på lab data for å forbedre simuleringene. Simuleringsresultatene vil bli målt opp mot data fra lab forsøk.

Gjennom rapport arbeidet har en stor grad av simuleringsutviklingen foregått selvstendig. I tillegg har et stort fokus blitt lagt på å tilegne meg kunnskap innen vibrasjoner og demping, noe som var et nytt emne for meg. Personlig deltakelse i impulsrespons forsøk utført hos Sandvik Teeness i Trondheim, ga meg viktig innsikt i dataene som parameterjustering og validering av simuleringene har blitt basert på.

Laboratorie og simuleringresultat ble sammenlignet i deres frekvensrespons. Simuleringsresultatenes magnitudo plottes basert på amplituden systemet svinger med når en harmonisk forstyrrelseslast virker på systemet, lastes påføres over et forhåndsdefinert frekvensområde i diskrete trinn. Laboratorie resultatene ble prosessert av Sandvik utifra målinger etter impulstester, og sendt over som frekvens respons med reel og imaginær part, hvor jeg så har plottet den respektive tilhørende magnitudo. På denne måten har jeg kunnet sammenligne resultater fra laboratorie og simulering.

Etter justering av gummi materialets parametre basert på passende data fra laboratorieforsøkene, ga simuleringene overraskende gode resultater, både når det gjelder nøyaktigheten til frekvens og magnitudo. Simuleringenes evne til å estimere frekvensverdi på magnitudetopper funnet i labforsøkene er veldig god, med mindre enn 4% feilmargin. Magnitudenøyaktighet med tanke på amplituden ble satt som en sekundær prioritet, men simuleringen treffer ganske bra også her, med en gjennomsnittlig feilmargin på 73% i forhold til de målte magnitudetoppene. Skalering av simuleringsmagnituden basert på den første toppverdien i lab- og simuleringresultatene, reduserte den gjennomsnittlige feilmarginen til 60%.

I lys av mål for oppgaven, sees rapporten og arbeidet som en personlig suksess, og skaper et solid grunnlag for videre arbeid og utvikling. For å gi selskaper som Sandvik nytte av Comsol som et simuleringprogram, er det fortsatt mye arbeid å gjøre. forskjellige årsaker til feil må undersøkes, samt å kjøre simuleringer med en mer sofistikert matematisk modell som krever mer datakraft enn det som var innen min rekkevidde gjennom rapport arbeidet.

---

## 2 Acknowledgments

The thesis period has been challenging both in terms of learning a totally new field, vibrations and damping, and the software Comsol. Taking on a new subject with little to no previous knowledge in the field for the master's year, once again underlined the diverse range of problems the engineering toolbox enables us to solve. I want to direct a special thanks to my advisor: Knut Sørby, for providing guidelines, setting me in touch with Sandvik Teeness, and helping me in the new field of vibration and damping. I also want to direct a big gratitude towards Dan Östling for letting me come to Sandvik Teeness when he conducted the lab experiments, and for answering my questions about the lab result. Thanks to my family for being a great support and to my mom and dad for traveling up to celebrate the end of five years at NTNU with me and my friend's families. Finally, I want to thank my friends at the office for making my cumbersome days brighter with jokes and pranks, and most of all for having worse days with the thesis than me(at least in my imagination).

- Audun Ryland



---

# Table of Contents

<b>1</b>	<b>Abstract</b>	<b>i</b>
1.1	English/Engelsk . . . . .	i
1.2	Norwegian/Norsk . . . . .	ii
<b>2</b>	<b>Acknowledgments</b>	<b>iii</b>
	<b>List of Figures</b>	<b>vi</b>
	<b>List of Tables</b>	<b>viii</b>
<b>3</b>	<b>Introduction</b>	<b>1</b>
3.1	Background and Motivation . . . . .	1
3.2	Problem Statement . . . . .	1
3.3	Goals and Objectives . . . . .	1
3.4	Scope and Limitations . . . . .	3
3.5	Research Questions . . . . .	4
3.6	Thesis Structure . . . . .	5
<b>4</b>	<b>Theoretical Background and Literature Review</b>	<b>6</b>
4.1	Previous Work . . . . .	6
4.2	Finite Element Analysis (FEA) . . . . .	7
4.3	Natural/Eigenfrequencies . . . . .	17
4.4	Modeling Vibrations . . . . .	19
4.5	Vibrations in Machining . . . . .	24
4.6	Tuned Mass Dampers in Tool Holders for Internal Machining . . . . .	25
4.7	Constitutive Models for Rubber . . . . .	28
<b>5</b>	<b>Methodology</b>	<b>31</b>
5.1	Comsol Multiphysics Software . . . . .	31
5.2	Modeling and Simulation of Vibration Damped Tool Holders . . . . .	32
5.2.1	A general walk-thru of the final simulations . . . . .	32
5.2.2	Simplified TMD Comsol Simulation . . . . .	33
5.2.3	Simplified Boring Bar with TMD Comsol Simulation . . . . .	35
5.3	Lab Experiments at Sandvik Teeness . . . . .	38
5.4	Experimental Validation . . . . .	41
<b>6</b>	<b>Simulation and Lab Results</b>	<b>43</b>

---

6.1	TMD without oil . . . . .	43
6.2	Boring bar with TMD(without damping fluid) . . . . .	46
6.2.1	Free Length 10xD: 400mm . . . . .	47
6.2.2	Free Length 11xD: 440 mm . . . . .	48
6.2.3	Free Length 12xD: 480 mm . . . . .	49
6.2.4	Comparison of simulations and lab results based on peak values . . . . .	50
<b>7</b>	<b>Discussion</b>	<b>52</b>
7.1	Simulation and Lab Setup . . . . .	52
7.2	Parameter Tuning . . . . .	53
7.3	Interpretation of Simulation and Lab Results . . . . .	53
7.4	Goals and objectives . . . . .	54
7.5	Addressing Research Questions . . . . .	55
7.6	Implications of the results and my contribution . . . . .	56
<b>8</b>	<b>Conclusion</b>	<b>58</b>
8.1	Summary of Key Findings . . . . .	58
8.2	Further Work . . . . .	58
	<b>Bibliography</b>	<b>60</b>
	<b>Appendix</b>	<b>62</b>

---

## List of Figures

1	Smart Goals . . . . .	1
2	FEA Work Flow . . . . .	7
3	Element shapes and dimensions . . . . .	8
4	Statically Determinate VS Statically Indeterminate . . . . .	8
5	Single Degree of Freedom system . . . . .	17
6	Impulse and Free vibration of a Single Degree of Freedom system . . . . .	18
7	Under, Critically and Over Damped SDOF systems . . . . .	22
8	LPM of a Two-Mass system . . . . .	26
9	Rubber temperature shift . . . . .	29
10	Viscoelasticity . . . . .	29
11	Simulation assembly model of a TMD without viscous damping(section view) . . .	32
12	Boring bar(section view) simulation assembly model with TMD . . . . .	32
13	Comsol view of imported and partitioned geometry, TMD assembly . . . . .	34
14	Comsol view of imported and partitioned geometry, Boring bar assembly . . . . .	36
15	Impact Hammer . . . . .	39
16	Setup in test bench: TMD without oil and accelerometer under mid-length . . . . .	39
17	Setup in test bench: TMD without oil and accelerometer under end of damper mass	40
18	Setup in the lathe for impulse test of the boring bar with TMD(without damper fluid). An accelerometer at the tip of the free end . . . . .	40
19	Simplified TMD, Modeshapes . . . . .	44
20	Comparison between Lab and Simulation, TMD: Translation . . . . .	44
21	Comparison between Lab and Simulation, Simplified TMD translation, Corrected Simulation Magnitude based on first mode peak values(Scalar= 0.571) . . . . .	45
22	Comparison between Lab and Simulation, TMD: Translation and Rotation . . . . .	45
23	Comparison between Lab and Simulation, Simplified TMD translation and rotation, Corrected Simulation Magnitude based on first mode peak values(Scalar= 0.571) .	45
24	Lab: Frequency Response Function, Comparison of varying free length . . . . .	46
25	Simplified Boring bar with TMD, 400mm, Undamped Modeshapes . . . . .	47
26	Comparison between Lab and Simulation, Free Length: 400 mm . . . . .	47
27	Comparison between Lab and Simulation, Free Length: 400mm, Corrected Simula- tion Magnitude based on first mode peak values(Scalar= 1.688) . . . . .	47
28	Simplified Boring bar with TMD, 440mm, Undamped Modeshapes . . . . .	48
29	Comparison between Lab and Simulation, Free Length: 440mm . . . . .	48
30	Comparison between Lab and Simulation, Free Length: 440mm, Corrected Simula- tion Magnitude based on first mode peak values(Scalar= 1.536) . . . . .	48

---

31	Simplified Boring bar with TMD, 480mm, Undamped Modeshapes . . . . .	49
32	Comparison between Lab and Simulation, Free Length: 480mm . . . . .	49
33	Comparison between Lab and Simulation, Free Length: 480mm, Corrected Simulation Magnitude based on first mode peak values(Scalar= 2.391) . . . . .	49

---

## List of Tables

1	Material Model Families and Examples . . . . .	14
2	Simulated Undamped Eigenfrequencies (Simplified TMD simulation) . . . . .	43
3	Simulated Undamped Eigenfrequencies (Simplified Boring Bar, 400 mm) . . . . .	47
4	Simulated Undamped Eigenfrequencies (Simplified Boring Bar, 440 mm) . . . . .	48
5	Simulated Undamped Eigenfrequencies (Simplified Boring Bar, 480 mm) . . . . .	49
6	Comparison of lab and simulation peaks(Frequency) . . . . .	50
7	Comparison of lab and simulation peaks(Magnitude) . . . . .	51
8	Testing the linear relationship between force and displacement when using Neo-Hookean hyperelastic material model . . . . .	51

---

## 3 Introduction

### 3.1 Background and Motivation

As an analytical and detail-oriented individual with a strong inner drive to understand how systems work, mechanical engineering was a natural pathway for me. My experience as a CNC Operator, a mechanical engineering student, and an engineering intern constitutes my foundation for completing my thesis.

Vibration-dampened tool holders have always interested me. Since I started working with them as an apprentice, they have proved to be an efficient tool, increasing metal removal rates and removing vibrations in high L/D ratio operations. The difference when changing from an undampened tool holder to a dampened holder trying to eliminate vibrations truly lets the technology shine.

Among other courses, the introductory course TMM4135- in the element method enabled me with the fundamental tools needed to simulate Tuned Mass Dampers (TMD's) by the use of Finite Element Method (FEM) simulations and this way gain insight into key performance parameters and to furthermore, validate the simulations by lab experiments. The thesis has given me the possibility to enhance my theoretical knowledge in vibration and damping theory, as well as the opportunity to perform a highly appreciated practical lab part.

### 3.2 Problem Statement

Elements of a vibration-damped tool holder shall be modeled and simulated in COMSOL. Special emphasis is put on the simulation model for rubber and tuning of the rubber material model parameters to fit simulation results to lab experiments. The simulation results will be measured against real-world lab measurements.

### 3.3 Goals and Objectives

The goals and objectives for the thesis serve distinct purposes and have been set to function as a pathway throughout the project. Goals are high-level statements, broad, long-term, and generally qualitative. They shall provide a clear sense of direction and illustrate the overall aim of what the thesis is set to achieve. Objectives are specific and clear in terms of the exact intention/outcome, short-term, and generally quantitative(measurable) steps that help to attain the goals. Each goal has connected objectives with the sole purpose of ensuring progress and enabling project management with a systematic approach to reaching the goals (Asana 2023).

In order to develop the goals and objectives, the SMART principle has been applied (*Objectives and goals: SMART* 2023). Each letter S, M, A, R, and T stands for a parameter that should be included and evaluated during development. Although goals are more qualitative than objectives, the SMART principle is seen as a powerful tool as it ensures quality in key parameters, and it is, for instance, important to be specific for both broad goals concerning a larger part of the project as well as narrow objectives focused on smaller parts.



Figure 1: Smart Goals

Source: <https://cultivateadvisors.com/blog/5-steps-to-writing-smart-business-goals/>

- 
- Specific
    - What shall be accomplished?
    - Point out a straight line to the final goal
    - Make sure that the goal is clear and concise
  - Measurable
    - Define the metrics of your goal
    - Set your goal in terms of the defined metrics enabling evaluation of success
  - Achievable
    - Make the Goal realistic
    - How will the available resources be managed to reach the goal?
  - Relevant
    - Make sure that the goals are connected with the vision and have solid backing in objectives
    - Ensure that the goal fits in with the problem statement
  - Time-Bond
    - Set a precise deadline for your goals. In order to reach the goals, objectives with due dates can be used as a tool on the way

Goals and Objectives:

- Set up a full simulation of a boring bar assembly with a TMD and have it run a frequency domain study before the end of the thesis
  - Max eigenfrequency deviation 5%
  - Using a material model adequately describing rubber and finding the correct parameters and values to meet the eigenfrequency deviation
  - Uncertainties connected to rubber material parameters and contact modeling can make it difficult to perform well on both frequency and amplitude accuracy. Due to peak frequency accuracy being of high priority, tuning for amplitude correlation should be done with visual control, reducing the time needed for tuning. Tuning for amplitude should give a curve following the same shape as the lab results.
- Perform real-life lab experiments to get data for validation and tuning of rubber material model.
  - Complete the experiments two months before the submission deadline of the thesis work in order to have the data ready when the simulations are ready to start parameter tuning.

---

### 3.4 Scope and Limitations

In this chapter, the scope and limitations of the thesis are presented. The scope defines the boundaries of the research, explaining what will be covered, while the limitations address the constraints and potential weaknesses of the study. Identifying the scope and limitations helps to set realistic expectations for the research and sheds light on areas for future investigation that won't be covered or taken into consideration in this thesis.

**Scope** The scope of this thesis is centered around the following aspects:

1. Focus on vibration-damped tool holders for internal turning operations: The research will concentrate on the development and simulation of vibration-damped tool holders specifically designed for internal turning operations.
2. Material properties and constitutive models for rubber: The study will emphasize the accurate representation of rubber materials in the finite element model, considering their specific properties and constitutive models.
3. COMSOL Multiphysics for finite element simulations: The research will utilize the COMSOL Multiphysics software for developing, simulating, and analyzing the finite element models of the vibration-damped tool holders without viscous damping.
4. Validation through experimental testing: The constitutive rubber model will be tuned using experimental data collected from laboratory tests performed on a tuned mass damper without viscous damping and on a full assembly with the TMD installed in a boring bar, still without viscous damping. The lab experiments will be used for simulation validation.
5. Parameter identification: The study will put special emphasis on finding key performance parameters in the rubber constitutive model and detecting how changes in the key performance parameters affect the simulation results of vibration-damped tools.

**Limitations** Due to the complexity of the scope, limitations exist that may impact the research outcomes. These limitations are important to acknowledge as they may influence the interpretation of the results and provide areas for future investigation:

1. Software limitations: The use of COMSOL Multiphysics for modeling and simulation inherently comes with some limitations and assumptions in the software's built-in material models and numerical methods, along with specific simulation decisions used in the modeling. These limitations might affect the accuracy of the results.
2. Experimental constraints: The laboratory experiments conducted to provide real-world results and to validate the simulation results are subject to measurement errors, due to noise, accuracy, and repeatability.
3. Material property simplifications: Constitutive models used for steel and rubber involve simplifications and assumptions that do not entirely capture the real-world behavior of the materials, potentially affecting the accuracy of the simulation results.
4. Time and knowledge constraints: Due to the limited time available for completing the thesis, certain aspects of the research may not be explored in-depth, which could impact the comprehensiveness of the study, along with the lack of knowledge on specific subjects and aspects of the thesis.

By acknowledging these limitations, the research can be better understood within its specific context, and potential areas for further investigation can be identified. The results and conclusions drawn from this thesis should be interpreted with the limitations in mind. Future research can build upon this work by addressing these limitations, exploring new materials, expanding the scope to different tool holders, or including more physical aspects such as viscous damping effects. As such, this thesis serves as a foundation for further investigations and advancements in the field of vibration-damped tool holders for internal turning operations, and simulation of TMDs.



---

### 3.5 Research Questions

This chapter presents the research questions that guide the focus and direction of the thesis. These questions help frame the investigation, ensuring that the research remains relevant and addresses the problem statement. By answering these research questions, the thesis aims to contribute valuable knowledge and insights to the scope of the thesis.

#### Main Research Question

The main research question addresses the core issue of the thesis and serves as the foundation for the subsequent sub-questions:

How can a finite element model of a vibration-damped tool holder for internal turning operations be developed and validated using COMSOL Multiphysics, focusing on accurately representing and tuning the behavior of rubber to return simulation results close to real-world behavior?

#### Sub-Research Questions

Several sub-research questions have been formulated to explore specific aspects of the problem in greater detail:

What are the key material properties and constitutive models of rubber that need to be considered for accurately modeling their behavior in a vibration-damped tool holder?

How can the finite element model of the vibration-damped tool holder be optimized to improve its accuracy and computational efficiency, considering the complexities of the materials involved?

What experimental methodologies and techniques can be employed to validate the simulation results obtained from the COMSOL Multiphysics model, ensuring the reliability and accuracy of the findings?

How do the results of the finite element simulations and experimental validation conform, and which parameters are best used to tune the rubber constitutive model?

By addressing these sub-research questions, the thesis aims to provide a comprehensive understanding of the modeling, simulation, parameter tuning, and validation process for vibration-damped tool holders. This information can contribute to a better understanding of tool holders for internal turning operations and key parameters, with the ultimate purpose of enhancing the performance of these tools in various industrial applications.

---

## 3.6 Thesis Structure

The thesis structure chapter provides an overview of the organization and layout of the thesis document. It serves as a roadmap for the reader, outlining the main sections and sub-sections, and briefly describing the content of each chapter. This overview is made to guide the reader through the research process, clarifying the logical flow of the thesis and the development of ideas.

### Overview of Thesis Structure

The thesis is organized into the following parts and chapters:

1. **Introduction:** Presents the background and motivation for the research, the problem statement, and the goals and objectives of the study. It also introduces the research questions that guide the focus and direction of the thesis.
2. **Theoretical background and Literature Review:** Reviews relevant theoretical background and literature in the field of vibration-damped tool holders, finite element modeling, and material modeling. It discusses key concepts, theories, and previous research, providing a comprehensive context for the study.
3. **Methodology:** Details the research methods employed in the thesis, including the development of the finite element model, the simulation process using COMSOL Multiphysics, simulation tuning, and experimental validation techniques. It also discusses the data collection and analysis procedures, ensuring the research is conducted systematically and rigorously.
4. **Simulation and Lab Results:** Presents the findings from the finite element simulations and experimental validation. It provides a detailed analysis of the results, including the effects of various parameters on the performance of the vibration-damped tool holders.
5. **Discussion:** This chapter interprets the results and draws connections between the findings and the existing literature. It addresses the research questions, discusses the implications of the results, and identifies any limitations or potential sources of error in the study.
6. **Conclusion:** Summarizes the main findings of the thesis, highlighting the contributions to the field of vibration-damped tool holders for internal turning operations. It also discusses the practical applications of the research and suggests areas for future investigation.
7. **References:** Lists all the sources cited throughout the thesis.
8. **Appendices:** Includes any supplementary materials.

---

## 4 Theoretical Background and Literature Review

This chapter contains the theoretical foundations of the research gathered from relevant literature. It includes the finite element method, mechanical vibrations, tuned mass dampers, and constitutive models for rubber.

### 4.1 Previous Work

Throughout my autumn semester thesis and this master's thesis, I have done simulations in Comsol Multiphysics of increasing complexity by taking the following steps in simulations. The workload and problem-solving behind each and every step have been an essential and dominating part of the thesis work, represented by the final simulations presented in the result section of the thesis. Number 1-10 was conducted in the autumn semester thesis and 11-13 during this master's thesis.

1. Beam Physics: Stationary deflection and stress analysis (2D)
2. Solid Mechanics: Stationary deflection and stress analysis (3D)
3. Beam Physics: Eigenfrequency study (2D)
4. Solid Mechanics: Eigenfrequency study (3D)
5. Beam Physics: Harmonic forced vibrations, Frequency domain, Modal (2D)
6. Solid Mechanics: Harmonic forced vibrations, Frequency domain, Modal (3D)
7. Solid Mechanics: Periodic forced vibrations, Frequency domain, Modal (3D)
8. Beam-Physics-Lumped-Mechanics: Various static and dynamic analysis (0D-2D)
9. Solid Mechanics: Periodic forced vibrations, Frequency domain, Modal (0D-3D)
10. Solid Mechanics: Assembly of steel-rubber-steel, Static, and dynamic analysis (3D)
11. Laminar Flow: Static analysis (2D)
12. Solid Mechanics: Rubber-steel-rubber assembly (to be described further in methodology, results, and discussion)
13. Solid Mechanics: Final assembly analysis (to be described further in methodology, results, and discussion)

---

## 4.2 Finite Element Analysis (FEA)

The Finite Element Method (FEM) is a numerical method used to solve complex mathematical problems in engineering and physics. The method involves dividing a complex system into smaller, simpler parts called elements. These elements are then analyzed using numerical methods. FEM analysis involves a great number of possibilities in attacking different problems and requires a solid understanding of different approaches in order to gain valid results and interpret the simulation results.

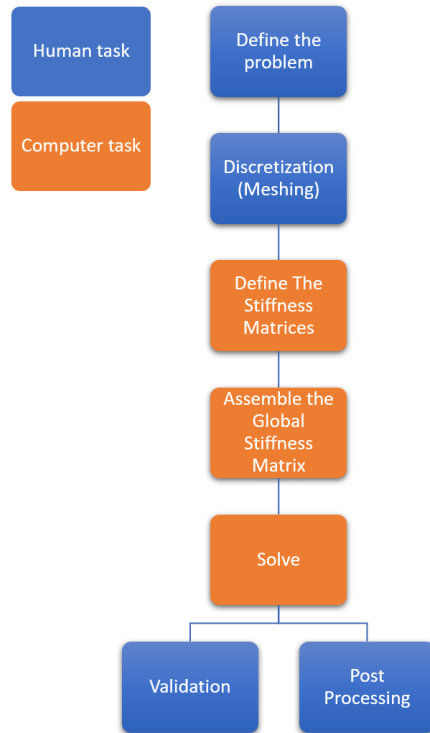


Figure 2: FEA Work Flow

Each of the element variations is assumed to behave in a specific way, determined by its shape, material properties, and boundary conditions. The behavior of each element is then modeled using mathematical equations that describe its response to external loads and boundary conditions.

The FEM involves discretizing the system into a finite number of elements, each defined by a set of nodes. Nodes are points within the element where the equations describing the behavior of the element are evaluated. The elements can be of one (beam), two (shell), or three (solid) dimensional form giving the nodes, respectively, two, four, and six degrees of freedom. The elements can further be of higher orders giving elements a greater number of nodes (the bottom row in Fig.3) (Ph.D 2019).

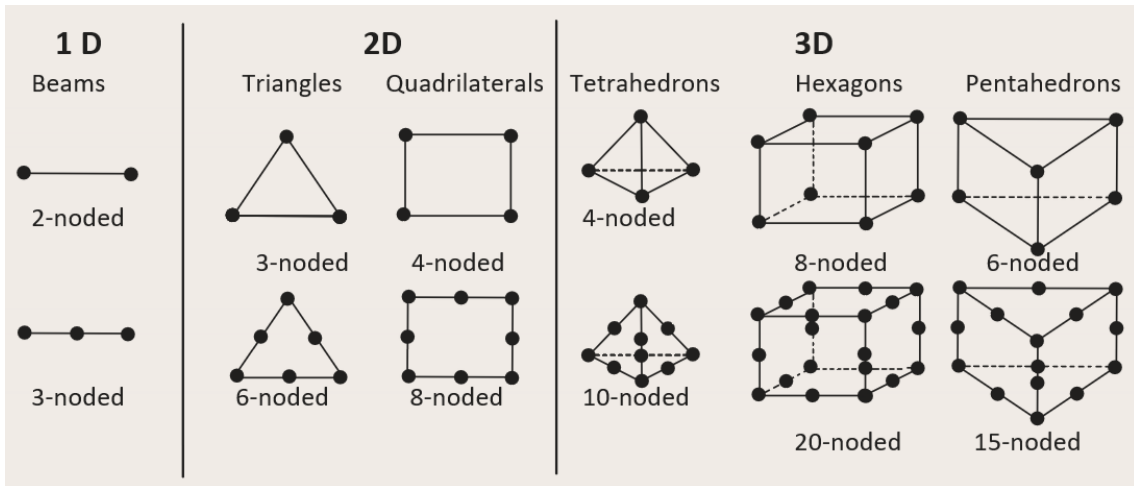


Figure 3: Element shapes and dimensions

The equations calculated at the individual nodes are further combined, forming a global system of equations describing the behavior of the entire system. Depending on the scope of the calculations, the equations can be set up to solve a widespread area of physics such as Solid Mechanics, Fluid Mechanics, Heat Transfer, Electromagnetic analysis, and more. In this chapter, the focus will be on Solid Mechanics, particularly Static, dynamic, and modal analysis.

In solid mechanics, also known as structural mechanics, you compute deformations, stresses, and strains. It is a field of applied mechanics where the objective often is to determine a structure's strength, such as a bike frame. Identifying dynamic properties such as eigenfrequencies, and time-dependent load responses, as well as flexibilities of a structure are also normal objectives.

Material science plays an important role in the computation of solid mechanics, as it is necessary to mathematically model the material behavior correctly. The models describing different materials vary greatly between different materials, for instance, metals, fluid, and rubber.

Concerning mechanics structures can be **statically determinate** or **statically indeterminate**. In the first case, all forces in the system can be calculated purely in terms of equilibrium. Static uncertainties are common in practice, at least when it comes to calculating the distribution of residual stresses in components. In statically uncertain systems, deformation must be considered in order to calculate forces.

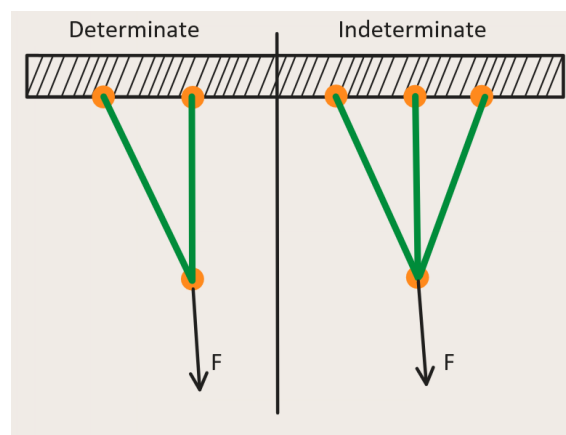


Figure 4: Statically Determinate VS Statically Indeterminate

The force of the two bars can be determined from the horizontal and vertical force balance of the force at the common joint in the determinate structure.

---

In the indeterminate structure the forces on the three rods cannot be determined solely by the balance of the two forces at the joint. Force distribution is affected by the stiffness of each bar.

Static Indeterminacy causes almost all solid mechanics analyses to rely on the same set of equation types: *equilibrium*, *compatibility*, and *constitutive relations* but they may appear in different forms, dependent on the analysis being at a continuum level or at a large-scale structural level (Comsol 2017).

**Stress and Equilibrium** Newton's second law forms the basis of the equilibrium equations. It states that all forces acting on a body including inertial forces, sum to a total of zero, meaning that all parts of a given structure must be in an equilibrium state. Virtually cutting a part, the internal stresses in the cut must balance out the external forces.

Sett inn egen fig her!

In three-dimensional space, the stress within a material is described by the stress tensor, which can be expressed as:

$$\sigma = \begin{bmatrix} \sigma_{xx} & \sigma_{xy} & \sigma_{xz} \\ \sigma_{yx} & \sigma_{yy} & \sigma_{yz} \\ \sigma_{zx} & \sigma_{zy} & \sigma_{zz} \end{bmatrix} \quad (1)$$

The individual elements in the stress tensor represent a force component per unit area in the material. One index signifies the force component's direction, while the other index indicates the orientation of the normal to the surface where the force is applied. Moment equilibrium considerations makes the stress tensor symmetric, containing six independent values.

Newton's second law can be expressed in terms of stress:

$$\rho \frac{d^2 u}{dt^2} = \nabla \cdot \sigma + f \quad (2)$$

Where:

- $f$  is force per unit volume
- $\rho$  is the mass density, and
- $u$  is the displacement vector.

### Strain and Compatibility

Compatibility relations impose constraints on deformations. In the case of a structural framework, the endpoints of all members connected at a single point must undergo identical displacements in both magnitude and direction.

Within the material, local deformations are described by the strain, which represents the relative deformation. For the straightforward elongation of a bar, strain, denoted as  $\varepsilon$ , is determined by the ratio of the displacement,  $\Delta$ , to the initial length,  $L_0$ .

For a general 3D case, Strain is also modeled by a symmetric tensor,

$$\varepsilon = \begin{bmatrix} \varepsilon_{xx} & \varepsilon_{xy} & \varepsilon_{xz} \\ \varepsilon_{yx} & \varepsilon_{yy} & \varepsilon_{yz} \\ \varepsilon_{zx} & \varepsilon_{zy} & \varepsilon_{zz} \end{bmatrix} \quad (3)$$

The discrete elements are defined as derivatives of the displacements,

---


$$\begin{aligned}
\varepsilon_{xx} &= \frac{\partial u}{\partial x}, & \varepsilon_{yy} &= \frac{\partial v}{\partial y}, & \varepsilon_{zz} &= \frac{\partial w}{\partial z}, \\
\varepsilon_{xy} &= \varepsilon_{yx} = \frac{1}{2} \left( \frac{\partial u}{\partial y} + \frac{\partial v}{\partial x} \right), \\
\varepsilon_{xz} &= \varepsilon_{zx} = \frac{1}{2} \left( \frac{\partial u}{\partial z} + \frac{\partial w}{\partial x} \right), \\
\varepsilon_{yz} &= \varepsilon_{zy} = \frac{1}{2} \left( \frac{\partial v}{\partial z} + \frac{\partial w}{\partial y} \right).
\end{aligned} \tag{4}$$

Due to their origin in a displacement field, the strain tensor's components are unable to have random spatial distributions. The compatibility requirements for a continuum are generated as a result. These compatibility requirements are fundamentally geometric relations, whether they be applied at the structural or continuum levels. These requirements are fundamental, much like the equilibrium relations, and do not require any assumptions (Comsol 2023g).

**Constitutive Relations** A material model acting as a connection between force and deformation or stress and strain is known as a constitutive relation. Unlike the previous two sets of equations, constitutive relations are not based on first principles and are entirely empirical. At most, laws of thermodynamics, symmetry conditions, and similar arguments can provide constraints on the possible mathematical structures of material models.

Material models establish a relationship between stresses and strains mathematically. For some elastic materials, this relationship is unique. In certain cases, the relation also includes time derivatives, as seen in viscoelasticity, or a record of previous strains, as observed in plasticity.

For each specific material, it is essential to conduct experiments and subsequently fit the obtained data to an appropriate mathematical model to replicate their true behaviour for the study to be conducted.

**Linearly elastic materials** The most basic material model is linear elasticity, where stresses are directly proportional to strains. Meaning that the deflection of for instance a beam, is proportional to the load applied. In many cases, this material model is adequate.

Isotropic linear elastic materials can be described by two independent material constants, normally the modulus of elasticity (Young's modulus),  $E$ , and Poisson's ratio,  $\nu$ .

Hooke's law in relation to deformations of a solid linear elastic material includes stress and strain to remove the stiffness geometric dependency.

Taking a bar with a cross-section area:  $A$  and length:  $L$ , subjected to an axial force  $F$ :

Stress:

$$\sigma = \frac{F}{A} \tag{5}$$

Strain:

$$\varepsilon = \frac{\Delta L}{L_0} \tag{6}$$

Where:

- $\sigma$  is the stress (in Pascal, Pa)
- $F$  is the applied force (in Newtons, N)
- $A$  is the cross-sectional area (in square meters,  $m^2$ )
- $\varepsilon$  is a strain (the ratio of change in length to the original length, a scalar)
- $\Delta L$  is the change in length (in meters, m)

- 
- $L_0$  is the original length (in meters, m)

Hooke's Law, in terms of stress and strain, is given by the equation:

$$\sigma = E\varepsilon \quad (7)$$

This relationship states that the stress acting on a material is proportional to the strain experienced by the material, and this proportionality is Young's modulus (*What is Hooke's Law?* 2023).

Expressing the axial force by  $\varepsilon$ ,  $E$ ,  $A$ , and  $L$ :

$$F = \varepsilon EA \quad (8)$$

The shear modulus also known as the modulus of rigidity, ( $G$ ) is a measure of a material's rigidity given by the ratio of shear stress to shear strain, sometimes also referred to as the 2nd Lamé parameter  $\mu$ .

For isotropic materials, which exhibit the same mechanical properties in all directions, the relationship between Young's modulus and the shear modulus can be expressed using Poisson's ratio ( $\nu$ ). Typically, a bar under tension not only elongates but also contracts in the transverse direction. Poisson's ratio is a dimensionless quantity that gives the relationship between the strain in the transverse directions and the strain in the axial direction:

$$\nu = \frac{\varepsilon_{\text{transverse}}}{\varepsilon_{\text{axial}}} \quad (9)$$

The following formula gives the relationship between these material properties:

$$G = \frac{E}{2(1 + \nu)} \quad (10)$$

Where:

- $G$  is the shear modulus (in Pascals, Pa)
- $E$  is the modulus of elasticity or Young's modulus (in Pascals, Pa)
- $\nu$  is Poisson's ratio (dimensionless)

Bulk modulus ( $K$ ), which measures a material's incompressibility or resistance to uniform compression, is another essential material characteristic. It is described as the ratio of the relative volume drop caused by the infinitesimal pressure increase:

$$K = -V \frac{dP}{dV} \quad (11)$$

where:

- $V$  is the volume [ $\text{M}^3$ ]
- $P$  is the pressure [ $\text{Pa}$ ],

and the negative sign ensures that  $K$  is always a positive number (since an increase in pressure should result in a decrease in volume). In terms of Young's modulus ( $E$ ) and Poisson's ratio ( $\nu$ ), the bulk modulus can be expressed as:



---


$$K = \frac{E}{3(1 - 2\nu)} \quad (12)$$

The equations show the interdependence between the modulus of elasticity, the shear modulus, and the bulk modulus in isotropic materials. By knowing any two of these material properties ( $E$ ,  $G$ ,  $K$ , or  $\nu$ ), it is possible to calculate the other properties. This relationship is crucial for understanding the mechanical behavior of isotropic materials and can be used in the analysis and design of vibration-damped tool holders for internal turning operations. These properties directly influence how materials respond to various types of stress and strain which can alter the material's vibrational behaviour. In vibration applications with rubber elements such as vibration-damped tool holders.

**Vibration control:** During internal turning operations, vibrations can be generated due to various factors such as cutting forces, tool geometry, and material properties. These vibrations can negatively impact the surface finish, tool life, and dimensional accuracy of the workpiece. By understanding the relationship between  $E$ ,  $G$ , and  $\nu$  and their impact on parameters like stiffness and strength, engineers can take qualified material choices with optimized damping properties that ensure a good fit between all materials in the vibration-damped tool holder assembly, ultimately improving the overall machining performance.

**Stiffness and Strength affecting eigenvalues** Eigenvalues are associated with the vibration behavior of a structure or material, and they are related to the natural frequencies of the system also referred to as eigenfrequencies. Eigenfrequencies are frequencies that a structure will vibrate at after excitation and then be left to vibrate freely. Stiffness and strength are mechanical properties that influence the overall behavior of a material, they do not directly affect eigenvalues. However, they do play a role in the frequency response of a system.

In the context of structural dynamics or mechanical vibrations, the eigenvalue problem is typically formulated in terms of a structure's mass ( $M$ ) and stiffness ( $K$ ) matrices. The eigenvalues and eigenvectors of this problem determine the natural frequencies and mode shapes.

The stiffness ( $K$ ) and mass ( $M$ ) matrices are influenced by the material's properties, such as its modulus of elasticity (stiffness) and density (mass). As the stiffness of a material increases, the overall stiffness of the structure tends to increase as well. This can result in higher eigenfrequencies. A structure's eigenfrequencies can be important for avoiding resonance or meeting specific design requirements related to vibration performance and are a big concern in the construction of large buildings and bridges.

Strength, on the other hand, is essential for ensuring that a structure or material can withstand the stresses induced by vibrations without yielding or failing. While it doesn't directly influence the eigenvalues, it plays a vital role in the overall durability and integrity of a structure subjected to dynamic loads.

Understanding the relationship between material properties like stiffness and strength and their impact on the vibration behavior of structures is crucial for the design and analysis of systems subjected to dynamic loads, to ensure structural integrity and functionality.

The 3D generalization of Hooke's law can be expressed as:

$$\begin{bmatrix} \sigma_{xx} \\ \sigma_{yy} \\ \sigma_{zz} \\ \sigma_{xy} \\ \sigma_{yz} \\ \sigma_{xz} \end{bmatrix} = \mathbf{D} \cdot \begin{bmatrix} \varepsilon_{xx} \\ \varepsilon_{yy} \\ \varepsilon_{zz} \\ \varepsilon_{xy} \\ \varepsilon_{yz} \\ \varepsilon_{xz} \end{bmatrix} \quad (13)$$

$D$  is a symmetric  $6 \times 6$  matrix containing 21 independent constants, Presented in a most general anisotropic case. For the isotropic case, it is only a function of  $E$  and  $\nu$ :

---


$$\mathbf{D} = \frac{E}{(1+\nu)(1-2\nu)} \begin{bmatrix} 1-\nu & \nu & \nu & 0 & 0 & 0 \\ \nu & 1-\nu & \nu & 0 & 0 & 0 \\ \nu & \nu & 1-\nu & 0 & 0 & 0 \\ 0 & 0 & 0 & \frac{1-2\nu}{2} & 0 & 0 \\ 0 & 0 & 0 & 0 & \frac{1-2\nu}{2} & 0 \\ 0 & 0 & 0 & 0 & 0 & \frac{1-2\nu}{2} \end{bmatrix} \quad (14)$$

The stiffness matrix,  $\mathbf{K}$ , is a key component of the FEM. The stiffness matrix relates the forces applied to the system to the displacements of the nodes. The stiffness matrix is calculated by integrating the element stiffness matrices for each element in the system. The element stiffness matrix,  $\mathbf{K}_e$ , is calculated using the following formula:

$$\mathbf{K}_e = \int_{\Omega_e} \mathbf{B}_e^T \mathbf{D}_e \mathbf{B}_e d\Omega \quad (15)$$

where  $\Omega_e$  is the domain of the element,  $\mathbf{B}_e$  is the strain-displacement matrix for the element, and  $\mathbf{D}_e$  is the constitutive matrix for the material.

The force vector,  $\mathbf{f}$ , is also a key component of the FEM. The force vector represents the external loads applied to the system. The force vector is calculated by summing the forces applied to each node in the system.

The displacement vector,  $\mathbf{u}$ , represents the displacement of each node in the system. The displacement vector is calculated by solving the global system of equations:

$$\mathbf{K}\mathbf{u} = \mathbf{f} \quad (16)$$

where  $\mathbf{u}$  is the displacement vector,  $\mathbf{K}$  is the stiffness matrix, and  $\mathbf{f}$  is the force vector.

In conclusion, the Finite Element Method is a powerful tool for solving complex mathematical problems in engineering and physics. The method involves dividing a complex system into smaller, simpler parts called elements, and then modeling the behavior of each element using mathematical equations. The FEM has many practical applications, including structural analysis(including vibration), heat transfer analysis, and fluid flow analysis.

FEA can be used to determine the natural frequencies, mode shapes, and response of a structure to external loads, making it a powerful tool in vibration analysis.

The natural frequencies of a structure can be calculated using the following formula:

$$f_n = \frac{1}{2\pi} \sqrt{\frac{k}{m}} \quad (17)$$

where  $f_n$  is the natural frequency,  $k$  is the stiffness of the structure, and  $m$  is the mass of the structure. The mode shapes of the structure can also be determined using FEA. Mode shapes describe the shape of the structure as it vibrates at different natural frequencies. The mode shapes are represented as vectors and can be expressed as:

$$\boldsymbol{\phi} = [\boldsymbol{\phi}_1, \boldsymbol{\phi}_2, \dots, \boldsymbol{\phi}_n] \quad (18)$$

where  $\boldsymbol{\phi}_i$  is the mode shape vector for the  $i^{th}$  natural frequency.

FEA can also be used to determine the response of a structure to external loads. The response of a structure can be calculated using the following equation:

$$\mathbf{u} = \mathbf{K}^{-1} \mathbf{f} \quad (19)$$


---

where  $\mathbf{u}$  is the displacement vector,  $\mathbf{K}$  is the stiffness matrix, and  $\mathbf{f}$  is the force vector. *The stiffness matrix and force vector are determined using FEA.*

## Material Models

There are various families of material models for structural mechanics applications, and each family contains several possible models. Below is a table listing a few examples<sup>1</sup>.

Material Model Family	Fam-	Examples	Common Material Models
Linear elastic		Many materials at small strains, e.g., metals	<ul style="list-style-type: none"> <li>• Hooke's law</li> <li>• Isotropic and anisotropic</li> </ul>
Elastoplastic, volume-preserving	volume-	Metals at larger strains	<ul style="list-style-type: none"> <li>• Tresca</li> <li>• von Mises</li> </ul>
Elastoplastic, stress-dependent	mean	Soils	<ul style="list-style-type: none"> <li>• Mohr-Coulomb</li> <li>• Drucker-Prager</li> </ul>
Creep		Metals at elevated temperatures	<ul style="list-style-type: none"> <li>• Norton</li> <li>• Garofalo</li> </ul>
Hyperelastic		Rubbers, biological tissues	<ul style="list-style-type: none"> <li>• Neo-Hookean</li> <li>• Mooney-Rivlin</li> </ul>
Viscoelastic		Plastics, Rubbers	<ul style="list-style-type: none"> <li>• Maxwell</li> <li>• Kelvin</li> <li>• Standard linear solid</li> </ul>

Table 1: Material Model Families and Examples

This table provides an overview of several material model families and examples of materials and common models within each family.

## Boundary Conditions

To adequately address the solid mechanics problem, it is necessary to apply appropriate boundary conditions. Assumptions are often made to make models less computationally heavy, and it is important to have a solid understanding of the impacts on the simulation results in order to ensure valid simulations. creating solid connections, contact pairs, spring connections, different combinations of translation and rotation conditions, and other boundary conditions must be done with caution.

## Defined Displacements

In some instances, the displacements are predetermined for certain portions of the body's boundaries, such as a structure resting upon the ground. If these known displacements do not adequately restrict all potential rigid body motions, determining the displacement field becomes unattainable. When external loads are recognized, it might still be feasible to compute stresses since absolute displacements may not be crucial. However, numerical solutions usually require a sufficient collection of defined displacements.

Mathematically, defined displacements correspond to Dirichlet conditions (A. H. .-. Cheng and D. T. Cheng 2005).

## Forces

External forces are commonly included in the formulation of solid mechanics problems.

Forces can take on a volumetric nature, such as gravity or centrifugal forces, which are integrated into the governing PDE rather than being considered boundary conditions.

On the contrary, there are loads that act on the boundaries, like the internal pressure within a pipe

---

or snow weight on a roof. These forces exemplify true Neumann boundary conditions (Venkateshan and Swaminathan 2014). In some scenarios, the orientation of the load shifts with the deformation termed a follower load. This results in a nonlinear problem since the load causes deformation, which then modifies the load.

### **Springs**

Elastic foundations can be regarded as a combination of the previous types, in which the force exerted on the structure is reliant on the displacement. They are frequently proportional, and from a mathematical standpoint, this constitutes a Robin boundary condition (Venkateshan and Swaminathan 2014). As an illustration, the ground beneath a building may not consistently be assumed to exhibit zero displacement, so its flexibility must be factored in accordingly. Elastic supports act as an alternative to defined displacements when mitigating rigid body movements.

### **Steady-state and Dynamic Problems**

Inertial forces arising from acceleration are included in the general form of Newton's second law. Often, loads exhibit slow variations, permitting the exclusion of dynamic terms. This supposition is widely employed in real-world engineering situations. A formulation of this nature is known as steady-state, stationary, or quasi-static.

### **Natural Frequencies**

Every structure possesses mass. When inertia and elasticity are combined through Newton's second law, it results in differential equations with second-order time derivatives. Navier's equations, mentioned earlier, are an example of this. The solutions to these equations typically resemble waves. The resulting equation system creates an eigenvalue problem when appropriate boundary conditions are used and a harmonic solution is assumed. A set of eigenvalues, sometimes referred to as natural frequencies or eigenfrequencies, are produced by solving this issue (Comsol 2023a=.

Physically, this implies that an elastic structure has a predisposition to oscillate at specific, distinct frequencies. For each natural frequency, the corresponding deformation pattern of the structure is known as an eigenmode.

Identifying a structure's natural frequencies is crucial to nearly all dynamic analyses, as it reveals the frequencies at which resonances might occur. Understanding the natural frequencies allows for determining whether a specific load's time scale can cause dynamic amplification. Throughout history, the catastrophic results of resonance caused by natural phenomena like the wind have made its impact by tearing down buildings and bridges like the Tacoma Narrows bridge (Practical Engineering 2018).

### **Dynamic Loading**

If loads exhibit a time variation with a time scale comparable to the period of some natural frequencies of a structure, accounting for the dynamic response becomes necessary. Dynamic loads fall into the categorization as deterministic and random loads. Deterministic loads involve completely known load histories affecting the structure, which is often seen in machine components. On the contrary, random loads do not have a predictable time history, except sometimes on the average value. Examples of random loads include wind loads and earthquake loads (Practical Engineering 2018).

### **Time-Varying Loads**

The most comprehensive description of a deterministic load involves the full-time history. To calculate displacements and stresses, the governing differential equations must be solved alongside a suitable set of initial conditions. This is typically done numerically using a time-stepping algorithm.

### **Harmonic Loads**

It is common for loads to exhibit harmonic variations in practice, particularly in rotating machinery. If the structure demonstrates linear behavior, the response will also be harmonic once any initial transients have dissipated. Such problems can be efficiently solved in the frequency domain. When

---

the frequency of a harmonic load is near a structure's natural frequency, the response experiences significant amplification compared to a steady-state solution. At resonance, when the loading frequency exactly aligns with a natural frequency, the vibration amplitude can become extremely large. Displacements are highly dependent on and limited only by the structure's damping, which often is found to be low.

For harmonic loading, it is customary to examine the frequency response. This entails analyzing the response for numerous loading frequencies and presenting the results as a frequency response function (FRF).

In cases where the problem is nonlinear, such as when mechanical contact is present, the response will not be harmonic even if the loads are. Generally, these problems must be solved as time-dependent issues.

### **Random Loads**

An example of a random load is the wind load on a tall building. The average wind speed varies along the height of the structure, and there are also wind gusts with random intensity and duration. Moreover, gusts are not always synchronous when observing different areas of the building. If multiple measurements are available, a time-dependent analysis could be conducted for each measurement in theory. However, this approach does not account for future events, as they will not precisely replicate the measured instances.

In situations involving random loads, it is more appropriate to characterize the load through its statistical attributes. This characterization is typically provided as a power spectral density (PSD). The response to such loads, in terms of displacements or stresses, is then also expressed using statistical parameters.

Vibration analysis using FEA has been applied in various engineering fields, including mechanical, aerospace, and civil engineering. For example, in the field of mechanical engineering, vibration analysis has been used to analyze the response of machine components to external loads. In aerospace engineering, vibration analysis has been used to study the dynamic response of aircraft structures to aerodynamic loads (Branesh et al. 2020). In civil engineering, vibration analysis has been used to evaluate the response of buildings and bridges to seismic and wind loads.

Summarised, FEA is a powerful tool for vibration analysis of complex structures. The natural frequencies, mode shapes, and response of a structure to external loads can be determined using FEA. The accuracy and efficiency of FEA make it an essential tool for engineers and designers looking to optimize the performance of their products.

---

### 4.3 Natural/Eigenfrequencies

As mentioned earlier in the Chap.4.2, natural frequencies are a system's predetermined frequencies at which it will vibrate freely. In this subsection eigenfrequencies in relation to mechanical structures will be explained, but to a certain degree, some of the models are generic.

When a structure vibrates at a specific eigenfrequency, it adopts a particular shape known as the eigenmode. Eigenfrequency analysis reveals the mode shape but not the amplitude of the actual vibration. Determining the true magnitude of the deformation requires knowledge of the actual excitation and damping properties.

Identifying a structure's eigenfrequencies is a crucial aspect of structural engineering. including the goals:

- Ensuring that periodic excitations do not create resonances resulting in excessive stress or noise emission.
- Verifying the appropriateness of a quasistatic analysis for a structure based on high natural frequencies compared to the load's frequency content.
- Determine the best time step or frequency to use for the ensuing dynamic response study.
- Providing eigenmodes and eigenfrequencies for further analysis based on mode superposition.
- Gaining insight into how to design alterations can impact a specific eigenfrequency by examining its mode shape.
- Design and development of vibration-dampening components and assemblies like damped internal tool-holders.

**Single Degree of Freedom** Let's start by looking at the simplest form, a system containing a spring, representing elasticity, the ability to deform and return to its original shape after loading scenario, and a mass: The system can be seen in the figure below.

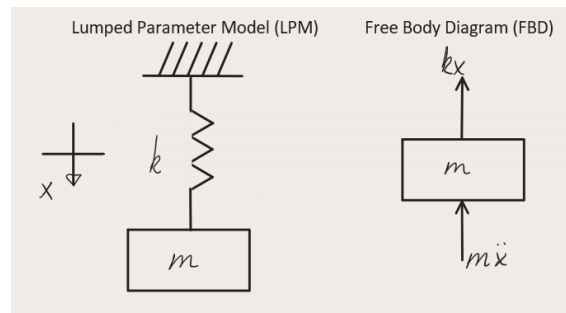


Figure 5: Single Degree of Freedom system

bodies that can be modeled as a mass and spring have three main scenarios: free vibration, forced vibration, and self-excited vibrations.

**Free Vibrations:** Unforced vibration takes place without the presence of a sustained external force. It arises due to certain initial conditions applied to the system, such as displacing it from its equilibrium position. Free vibration results in motion at one or more of the system's natural frequencies, and since every physical structure experiences some level of damping (energy dissipation), it appears as a diminishing oscillation with a relatively brief duration. Common examples include hitting a tuning fork or a springboard after a jump.'

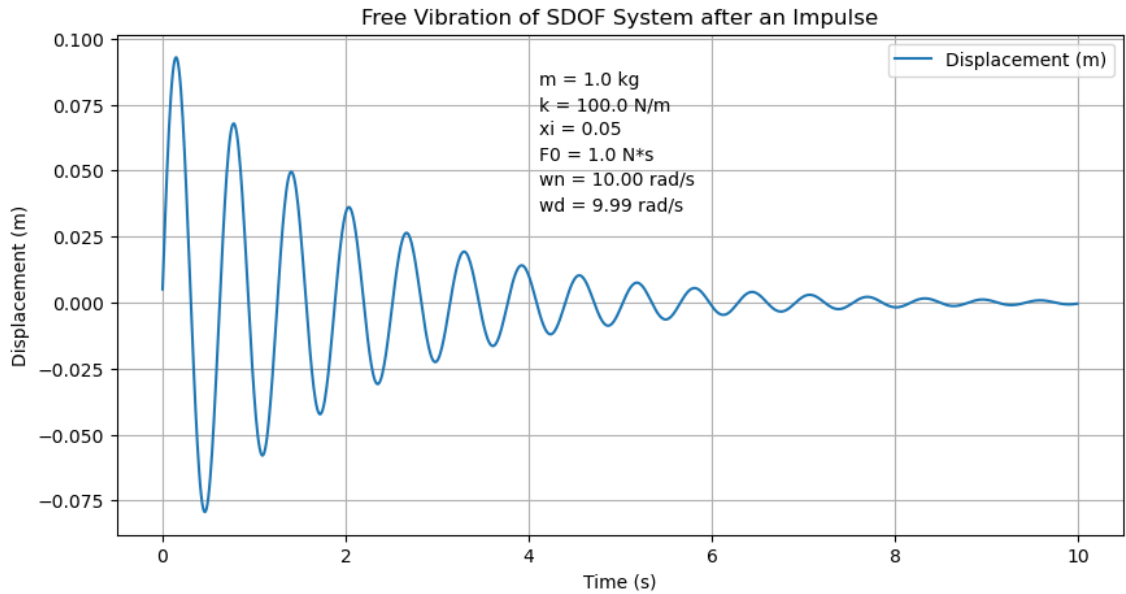


Figure 6: Impulse and Free vibration of a Single Degree of Freedom system

**Forced vibrations:** Induced vibration occurs when a persistent, external periodic force generates a response with the same frequency as the driving force (once initial transients have diminished). While free vibration is commonly depicted in the time domain, induced vibration is typically examined in the frequency domain. This highlights the magnitude and phase dependency on frequency, allowing for easy identification of natural frequencies. Rotating imbalance is a common cause of induced vibration in mechanical systems. Significant vibrations can take place when the excitation frequency,  $\omega$ , aligns with the system's natural frequencies,  $\omega_n$ , leading to resonance. Generally, resonance is to be avoided, in vibration damping, but some exceptions exist.

**Self Excited Vibrations** In self-excited vibration, a constant input force exists, similar to forced vibration. However, this input is transformed into vibrations at one of the system's natural frequencies, as observed in free vibration. Various physical mechanisms facilitate this modulation. Familiar instances of self-excited vibration: playing a violin, wing flutter in a flute, and chatter during machining processes.

In summary, all mechanical systems possess mass and are not infinitely rigid. Consequently, they are either stationary or vibrating. If the source of vibrational energy is only applied at the initiation of motion (like tapping a tuning fork), the resulting motion is a free vibration. Free vibrations occur at the natural frequency of the system. A higher natural frequency is achieved with increased stiffness or decreased mass, whereas a lower natural frequency occurs with reduced stiffness or increased mass. Using the tuning fork example, higher notes (higher frequencies) are produced by tight (stiff) and thin (low mass) fork arms, while lower notes (lower frequencies) are created by loose (less stiff) and thick (high mass) strings. In machine tools, low frequencies are experienced when the vibrating objects are heavy (like a machine tool's column) or flexible (like a long, slender workpiece), or both (Comsol 2023a).

---

## 4.4 Modeling Vibrations

Since modeling vibrations can be challenging, we begin by examining the single-degree-of-freedom free vibration in more detail using a simple, lumped parameter model. The mass-less spring in this model acts as the oscillating restoring force, and it is assumed that all the mass is concentrated at the coordinate location. The model is made up of a mass,  $m$ , attached to a linear spring,  $k$ , which produces a force proportional to the mass's displacement from its static equilibrium position. Since the rigid mass is constrained to move vertically, a single time-dependent coordinate,  $x$ , describes its motion completely. Understanding the movement of a single coordinate is enough to describe the motion of a single-degree-of-freedom (SDOF) system completely. Fig.5, includes the Lumped parameter model and free body diagram. Adding the spring and inertial forces acting in the vertically gives the equation of motion for the model (Schmitz and Smith 2019).

$$m\ddot{x} + kx = 0 \quad (20)$$

Assuming a harmonic solution of the form  $x = Xe^{st}$ , where  $X$  is a complex coefficient,  $s = i\omega$ , and  $\omega$  is the frequency (in rad/s), we can express the velocity as the first time derivative of the displacement,  $\dot{x} = sXe^{st} = i\omega Xe^{st}$ , and the acceleration as the second time derivative,  $\ddot{x} = s^2Xe^{st} = -\omega^2Xe^{st}$  (note that  $i = \sqrt{-1}$  and  $i^2 = -1$ ). Substituting into Eqn.20 yields:

$$Xe^{st}(ms^2 - k) = 0 \quad (21)$$

In this equation, either  $Xe^{st}$  or  $(ms^2 - k)$  must be zero. The trivial solution is when the first term is zero, which suggests that no motion has taken place. The scenario when the second term equals zero is the one that interests us. This is referred to as the system's characteristic equation:

$$ms^2 - k = 0 \quad (22)$$

Solving for the complex variable  $s$  gives the two roots  $s = \pm\sqrt{-\frac{k}{m}} = \pm i\sqrt{\frac{k}{m}}$ . The vibrating frequency  $\sqrt{\frac{k}{m}} = \omega_n$  is the natural frequency for the single-degree-of-freedom system. For  $k$  and  $m$ , N/m and kg are normal SI units, which results in units of rad/s for  $\omega_n$ . The natural frequency can be expressed in units of Hz (cycles/s) as well. In this case described by the notation  $f_n = \frac{\omega_n}{2\pi}$ .

Eqn.20 total solution is the sum of each of the two roots:

$$x = X_1e^{i\omega_n t} + X_2e^{-i\omega_n t} \quad (23)$$

$X_1$  and  $X_2$ , being the complex coefficients, can be determined from the initial displacement,  $x_0$ , and velocity,  $\dot{x}_0$ , in the SDOF system. Evaluating Eqn.23 at  $t = 0$  gives:

$$x_0 = X_1 + X_2 \quad (24)$$

The first time derivative of 23 is:

$$\dot{x} = i\omega_n X_1 e^{i\omega_n t} - i\omega_n X_2 e^{-i\omega_n t} \quad (25)$$

At  $t = 0$ , Eqn.25 becomes:

$$\dot{x}_0 = i\omega_n(X_1 - X_2) \quad (26)$$

Using the linear combination approach, Eqn.24 and 26 can be combined to determine the complex conjugate coefficients  $X_1$  and  $X_2$ :



---


$$X_1 = \frac{-i\dot{x}_0 + \omega_n x_0}{2\omega_n} \quad (27)$$

and

$$X_2 = \frac{i\dot{x}_0 + \omega_n x_0}{2\omega_n} \quad (28)$$

These coefficients can then be substituted in Eqn.23 to determine the time-dependent displacement of the mass due to the imposed initial conditions. A different way to express the mass motion is in exponential form. To use this notation, we must first determine which parts of the complex coefficients are real (Re) and imaginary (Im):

$$\begin{aligned} \text{Re}(X_1) &= \frac{x_0}{2} \\ \text{Im}(X_1) &= \frac{-\dot{x}_0}{2\omega_n} \end{aligned} \quad (29)$$

$$\begin{aligned} \text{Re}(X_2) &= \frac{x_0}{2} \\ \text{Im}(X_2) &= \frac{\dot{x}_0}{2\omega_n} \end{aligned} \quad (30)$$

Using the real and imaginary part to write the coefficients exponentially:

$$X_1 = Ae^{i\phi} = \sqrt{\left(\frac{x_0}{2}\right)^2 + \left(\frac{-\dot{x}_0}{2\omega_n}\right)^2} \cdot \exp\left[i \arctan \frac{-\dot{x}_0}{2\omega_n x_0}\right] \quad (31)$$

where the magnitude is  $A = \sqrt{\frac{x_0^2 \omega_n^2 + \dot{x}_0^2}{4\omega_n^2}}$  and the phase is  $\phi = \arctan \frac{-\dot{x}_0}{x_0 \omega_n}$ .

In the same way  $X_2 = Ae^{-i\phi}$  (same magnitude, but negative phase) due to it being the complex conjugate of  $X_1$ . Can then rewrite the total solution from Eqn:23 in the form:

$$x = Ae^{i(\phi + \omega_n t)} + Ae^{-i(\phi + \omega_n t)} = A \left( e^{i(\omega_n t + \phi)} + e^{-i(\omega_n t + \phi)} \right) \quad (32)$$

And then utilising the Euler identity:  $e^{i\theta} + e^{-i\theta} = 2 \cos(\theta)$ , Eqn.32 can be rewritten as:

$$x = 2A \cos(\omega_n t + \phi) \quad (33)$$

The equation 33 illustrates the oscillatory behavior of mass movement, revealing that the amplitude and phase are dependent on the initial conditions. To realistically represent physical systems, we must incorporate damping into our analysis. Damping is the process where part of the energy input into a vibrating system is "lost" or transformed, rather than contributing to motion. This means that not all energy input directly influences motion - some is dispersed through other channels, normally as heat. A detailed representation of damping can be complex and may not be ideally suited for integration into our simplistic mathematical interpretation of single-degree-of-freedom free vibration. Hence, typically one or more from three mathematically simplistic yet efficient damping models are employed.

**Viscous damping** Viscous damping is recognized as a common model in mechanical systems to represent the energy dissipation due to the system's motion. Frequently employed in the analysis of single-degree-of-freedom (SDOF) systems. Viscous damping is characterized by a linear relationship between the damping force and the system's velocity.

---

In viscous damping, a damping coefficient, denoted by 'c', represents the proportionality factor connecting the damping force ( $F_d$ ) and the velocity ( $\dot{x}$ ) of the system. Mathematically, the damping force can be expressed as:

$$F_d = c \cdot \dot{x} \quad (34)$$

The negative sign signifies that the damping force counteracts the motion of the system, functioning to diminish its velocity.

Concerning an SDOF system, the motion equation incorporating viscous damping can be described as:

$$m \cdot \ddot{x} + c \cdot \dot{x} + k \cdot x = 0 \quad (35)$$

where:

- $m$  is the mass of the system,
- $\ddot{x}$  is the acceleration,
- $c$  is the damping coefficient [N – s/m]
- $\dot{x}$  is the velocity,
- $k$  is the stiffness of the system, and
- $x$  is the displacement.

The damping ratio ( $\zeta$ ) is a dimensionless quantity that represents the ratio of the actual damping coefficient ( $c$ ) to the critical damping coefficient ( $c_c$ ), which is the minimum damping required to inhibit oscillatory behavior in the system. The damping ratio can be described as:

$$\zeta = \frac{c}{c_c} \quad (36)$$

Based on the damping ratio value, the system's behavior can be divided into three categories:

1. Underdamped ( $\zeta < 1$ ): The system exhibits oscillatory behavior with a diminishing amplitude.
2. Critically damped ( $\zeta = 1$ ): The system returning to the equilibrium position in the fastest possible time period without any oscillation.
3. Overdamped ( $\zeta > 1$ ): The system returns to its equilibrium position without oscillating, but it takes a longer time compared to a critically damped system.

The three damping scenarios applied to a prescribed displacement that suddenly is removed can be seen in the plot from my Python script in Fig.7.

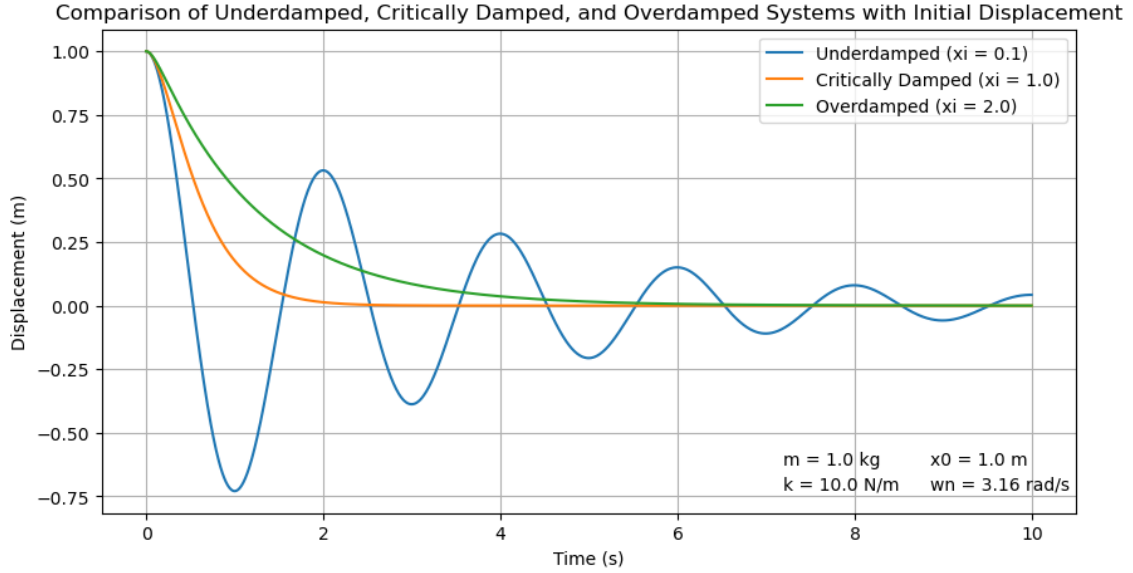


Figure 7: Under, Critically and Over Damped SDOF systems

Viscous damping is crucial in mechanical systems design as it aids in vibration control and reduces resonant frequencies effects, ensuring more stable and dependable performance. Since viscous damping is frequency dependent, the velocity can be expressed as:

$$v = \frac{dx}{dt} = \dot{x} = sXe^{st} = i\omega Xe^{st} \quad (37)$$

where:

- $s$  is a complex variable,  $s = i\omega$ , with  $\omega$  representing the frequency (in rad/s),
- $X$  is a complex coefficient, and
- $t$  is the time.

By examining the relationship between damping force and velocity, engineers can effectively design systems that minimize undesirable vibrations and increase the overall reliability of the system.

**Coulomb Damping:** Coulomb damping, also referred to as dry friction or sliding friction damping, is another essential damping model applied in mechanical systems. Unlike viscous damping, Coulomb damping is not frequency-dependent and exhibits a constant damping force that opposes the direction of the relative motion between the system components.

In Coulomb damping, the damping force ( $F_d$ ) remains constant regardless of the system's velocity ( $v$ ), and its mathematical expression is:

$$F_d = -\mu N \quad (38)$$

where:

- $\mu$  is the friction coefficient between the contacting surfaces, and
- $N$  is the normal force acting on the surfaces.

For an SDOF system with Coulomb damping, the motion equation can be written as:

---


$$m \cdot \ddot{x} + \mu N \cdot \frac{\dot{x}}{|\dot{x}|} + k \cdot x = 0 \quad (39)$$

where:

- $m$  is the mass of the system,
- $a$  is the acceleration,
- $\mu$  is the friction coefficient,
- $N$  is the normal force,
- $v$  is the velocity,
- $k$  is the stiffness of the system,
- $x$  is the displacement, and
- $\frac{\dot{x}}{|\dot{x}|}$  is the sign function, which returns the sign of the velocity.

Coulomb damping is particularly relevant in systems with components in sliding contact, such as brakes, clutches(dry), or any other application with dry friction between surfaces. Due to its constant nature, Coulomb damping can cause a system to exhibit stick-slip behavior, resulting in jerky and uneven motion. This behavior can be beneficial in specific applications, such as friction dampers for seismic protection sometimes installed in buildings, but may be undesirable in others.

By analyzing and incorporating Coulomb damping in mechanical system design, engineers can create systems that exhibit desired motion characteristics and effectively control vibrations, leading to improved system performance and stability.

**Solid Damping:** Material damping, also referred to as internal or structural damping, is a type of damping that occurs within the substance of a mechanical system due to energy dissipation within the material's composition. Material damping is a result of the internal friction between microscopic components of a material as it undergoes deformation. Considering material damping is vital in systems where energy dissipation within the substance plays a significant role.

For a single degree of freedom (SDOF) system with material damping, the equation of motion can be expressed as:

$$m \cdot \ddot{x} + c \cdot \dot{x} + k \cdot x + k \cdot \beta \cdot \dot{x} = 0 \quad (40)$$

where:

- $m$  is the mass of the system,
- $\ddot{x}$  is the acceleration,
- $c$  is the viscous damping coefficient,
- $\dot{x}$  is the velocity,
- $k$  is the stiffness of the system,
- $x$  is the displacement,
- $\beta$  is a dimensionless coefficient specific to the material damping,

---

In this equation, the term  $k \cdot \beta \cdot \dot{x}$  represents the material damping force, which is proportional to the system's velocity. This term captures the energy dissipation within the substance as the system vibrates.

It is important to note that material damping is frequency-dependent, and the rate of energy dissipation relies on the material properties and the rate of deformation. Some materials exhibit higher material damping than others, such as specific metal alloys and viscoelastic materials.

Taking material damping into account in mechanical system design enables engineers to optimize the system's dynamic performance and stability, resulting in more dependable and efficient operation.

## 4.5 Vibrations in Machining

Machining processes, such as milling, turning, and drilling, are essential manufacturing techniques and are applied to a wide spectrum of industries. These processes involve the removal of material from a workpiece and are known as subtractive manufacturing processes. Machining cells are in general low in damping and exposed to different types of vibrations. Vibrations normally have a negative effect on product quality, tool life, and overall productivity as well as affecting the work environment by loud noise. The complexity of machining vibration is high, and a large number of parameters are affecting the stability of the machining processes. Larger machines, as well as high precision machines, are connected to separate fundamentals in the ground, with the purpose of isolating them as much as possible from the space around them, with the purpose of restricting vibrations to travel in or out from the machining cell. This chapter aims to provide a theoretical background on vibrations in machining operations, in particular, internal turning operations with boring bars, and will discuss the different types of vibrations, their sources as well as their impact on machining performance.

Long boring bars for internal turning operations have low static and dynamic stiffness, making them prone to vibrations. Boring bars have traditionally been made of different variations of solid steel and tungsten carbide, providing better stability due to the increased modulus of elasticity, but at a higher price-point, boring bars of solid steel are normally used up to  $4xD$  ( $L/D=4$ ), and tungsten carbide up to  $7xD$ . As mentioned in paragraph 4.3 we divide vibrations in machining into three categories as well: free, forced, and self-excited vibrations (Sørby 2016).

**Free Vibrations:** Occurs due to forces externally affecting the machining structure, causing a deflection, and then ceasing, letting the system oscillate according to its dynamic properties at a frequency close to one of the eigenfrequencies until the vibrational energy dissipates. Free vibrations in turning operations can come from chippings jamming between the workpiece and boring bar, or from significant hard spots in the material. If a free vibration scenario plays out in a turning operation, it will leave distinct marks in the workpiece, and the vibrations will stop due to internal structure damping and damping at the contact surface between the cutting tool and the workpiece.

**Forced Vibrations:** Originates from periodically induced forces that in a turning operation may come from radial borings, splines, grooves, and other radial inconsistencies, but also from runout due to crooked fixturing and mismatch between clamping force and workpiece wall thickness, giving variations in cut-depth and thereby force. Periodic forces may also be applied to the system by an unevenly distributed mass in relation to the axis of rotation, creating vibrations. The structure exposed to the periodic forces will oscillate at the same frequency as the periodic force. After a given time period the system reaches equilibrium, also known as steady-state where the amplitude and frequency of the oscillations become constant.

**Self-excited Vibrations:** Chatter, also known as self-excited vibrations, is the most dominant and damaging group of vibrations in machining. Two major types of chatter are **regenerative** and **mode-coupling**.

**Regenerative chatter** comes into play when tool oscillations produce a wavy pattern on the surface of the workpiece, which is reproduced in the coming revolutions of the workpiece. The changes

---

in chip thickness rely on the phase difference between the wavy patterns in successive revolutions and therefore rely on the workpiece's rotational speed. A stability chart, which demonstrates the stability threshold of a machining process in relation to rotational speed, is normally utilized to pinpoint high stability for a large depth of cut.

**Mode-coupling chatter** oscillates elliptically with a variable engagement of the tool, oscillating between high and low engagement of the cutting tool making the cutting force larger and lower than the tool stiffness, making the tool vibrate in an elliptical matter. Mode coupling chatter can occur without interaction with a previously generated surface waviness, differentiating it from regenerative chatter where a waviness from a previous cut is regenerated in the next revolution. Mode coupling chatter can occur in some machining operations like thread cutting where the cutting edge can cut surfaces not cut at the previous revolution, and it is also seen in some operations with boring bars. Even though it is present in some machining operations, it is generally not included in chatter analysis in machining.

To sum up, vibrations in machining are generally a bad system behavior that we want to reduce. Long overhangs and small diameters are a bad combination in terms of avoiding vibrations. Internal turning operations are exposed to vibrations, this is due to a number of factors, some being: diameter limitations in order of leaving space for chip removal, operations, and products requiring high Length/Diameter ratios. By building a TMD (Tuned Mass Damper) into the tip of the boring bar the system stability and resistance against vibrations can be greatly increased.

## 4.6 Tuned Mass Dampers in Tool Holders for Internal Machining

Different means of active, semi-active, and passive methods exist in the world of machining and passive systems are dominant in magnitude. According to a representative from Sandvik Teeness, a problem with active damping in boring bars is the space that actuators and sensors take up, negatively affecting the stiffness and space left for maximizing the damping mass. Active damping is therefore more often seen as useful in the workpiece fixturing and includes sensor packages and actuators making the systems complex. Semi-active damping systems can also be found for instance by the use of a coil and magnetorheological fluid to adjust the viscosity of the damper fluid and by this being able to adjust the system parameters according to different scenarios. Tuned Mass Dampers are both relatively low-cost and highly efficient in providing high stability and resistance against vibrations while also being easy to use as a "plug and play" product for the customers. This has made the application of a tuned mass damper in the tip of the tool holder popular in the industry.

The tuned mass damper (TMD) consists of a damper mass, a spring, and a damper element. TMD's are tuned in different ways but to begin with, we can say that it is tuned to vibrate at the same frequency we want to suppress but out of phase so that the masses move in opposite directions.

Taking the passively damped boring bar with a tuned mass damper located at the free end as the subject, we can model it as a two-mass system with a spring and damper between both the masses and the fixed boundary.

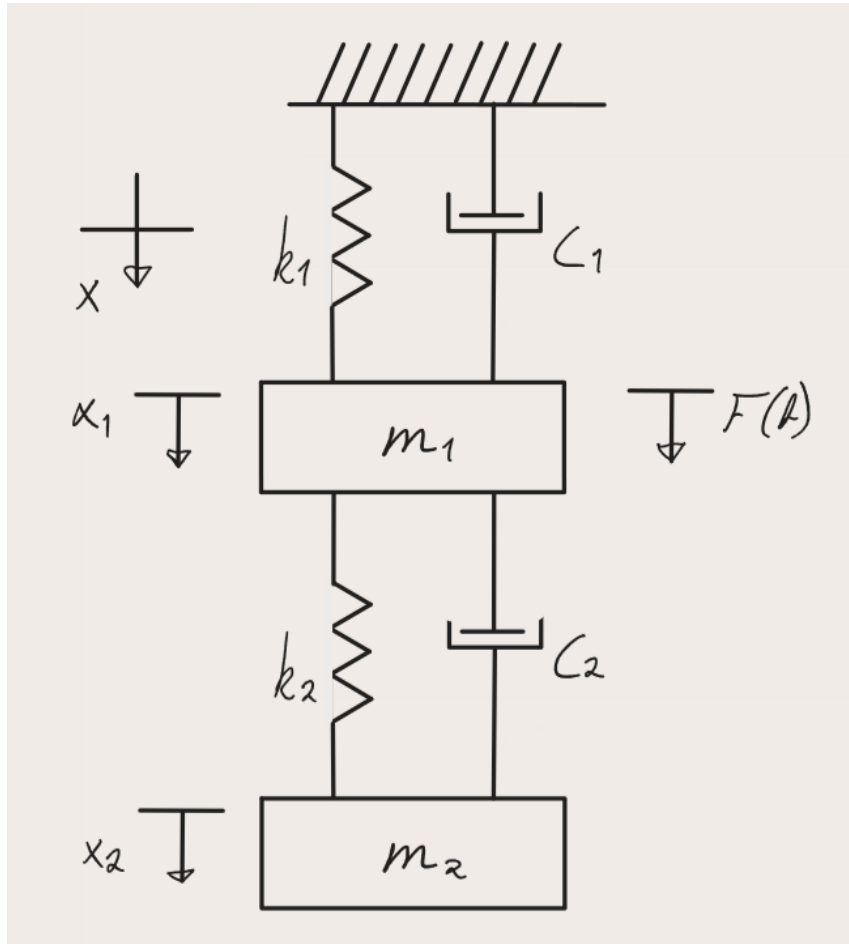


Figure 8: LPM of a Two-Mass system

Where:

- $m_1$ : is the mass of the bar
- $k_1$ : is the stiffness of the bar and connecting machine interface
- $c_1$ : is the internal damping in the bar and connecting machine interface
- $x_1$ : is the global displacement of  $m_1$
- $F(t)$ : is the force applied at the cutting edge over time
- $m_2$ : is the damper mass
- $k_2$ : is the stiffness of the connecting element between the damper mass and boring bar
- $c_2$ : is the internal damping of the damper mass, it consists of the damping in the connecting element between the damper mass and boring bar and the viscous damping
- $x_2$ : is the global displacement of  $m_2$

The equations of motion are (Schmitz and Smith 2019): For  $m_1$  :

$$m_1 \ddot{x}_1 + (c_1 + c_2) \dot{x}_1 + (k_1 + k_2) x_1 - c_2 \dot{x}_2 - k_2 x_2 = 0 \quad (41)$$

And for  $m_2$  :

$$m_2 \ddot{x}_2 - c_2 \dot{x}_1 - k_2 x_1 + c_2 \dot{x}_2 + k_2 x_2 = 0 \quad (42)$$

---

Normally the connecting element between the damper mass and the boring bar is a rubber element, and the geometry and material parameters decide the stiffness and damping provided. In order to look at the force response,  $F(t)$  is applied at the boring bar boundary  $m_1$ . When we get a force input via  $F(t)$ ,  $m_1$  will move, resulting in a deflection of the boring beam  $x_1$ . Depending on the system parameters, a change in the damper mass position  $x_2$  will take place. A TMD's effectiveness is dependent on two major factors: the tuning (the capability to vibrate at the same frequency as the primary structure), and its mass. TMD's purpose is to absorb the vibrational energy from the primary structure and transform it into other forms of energy, primarily heat. The ability to absorb energy is proportional to the weight of the damper mass, due to the ability to provide a greater reaction force to a relative displacement between the masses:  $abs(x_1 - x_2)$ . Due to this, high-density materials are often used, and the mass is placed at the location of max displacement during vibrations (the free end of a boring bar). A number of constraining factors can be relevant; space, structural integrity, weight constraints, and more, making it a classical engineering task of finding a suitable compromise for the best result.

The frequency response function for the system is based on the formulation:  $FRF \equiv \frac{Output}{Input} \Rightarrow H \equiv \frac{x_1}{F}$  is written:

$$H(j\omega) = \frac{k_2 - m_2\omega^2 + jc_2\omega}{A} \quad (43)$$

where:

$$A = -m_1m_2\omega^4 + (m_1c_2 + c_2m_2 + c_1m_2)j\omega^3 + (k_1m_2 + k_2m_2 + m_1k_2 + c_1c_2)\omega^2 - (k_1c_2 + c_1k_2)j\omega - k_1k_2 \quad (44)$$

After the selection of materials and size for the assembly, the tuning is next up. This is done by adjusting the spring stiffness, which together with the damper mass and fluid decides the eigenfrequency. Tuning is done based on the parameters  $k_2$  and  $c_2$ , finding the optimum solution. Depending on which vibration problem one targets to eliminate, two criteria for optimization are to be described: Minimized magnitude of FRF, and Maximized negative real part of the FRF. Both optimization methods are based on the Eqn.43

**Minimized magnitude of FRF:** The dominating method in the industry, and has the key feature of giving the shortest vibration intervals at free vibrations. When applied there will be two equally high peaks on the magnitude curve, and it is the optimal tuning when preventing forced vibrations at the eigenfrequency of the undamped boring bar. Using the optimization criteria will also reduce the self-excited vibrations caused by mode-coupling to a minimum, and these vibrations happen at the boring bar eigenfrequency. Due to the qualities of the minimized magnitude of FRF tuning criterium, it is ideal for turning when chips, material, or discontinued cuts per revolution result in impact forces. When performing the tuning, the optimal eigenfrequency and damping ratio for the TMD is found by the formulas (Den Hartog 1947):

$$\omega_{2,opt} = \frac{1}{1 + \mu}\omega_1 \quad (45)$$

$$\zeta_{2,opt} = \sqrt{\frac{3\mu}{8(1 + \mu)}} \quad (46)$$

Where:

- $\mu = \frac{m_2}{m_1}$
- $\omega_1 = \sqrt{\frac{k_1}{m_1}}$

After these calculations, Eqn.45 and 46, optimal spring stiffness,  $k_{2,opt}$  and damping coefficient,  $c_{2,opt}$  can be found by the equations:



- 
- $k_{2, \text{opt}} = \sqrt{\frac{k_{2, \text{opt}}}{m_2}}$
  - $\zeta_{2, \text{opt}} = \frac{c_{2, \text{opt}}}{(2m_2\omega_{2, \text{opt}})}$

**Maximized negative real part of the FRF** Has the key feature of giving the highest resistance to regenerative chatter, which also is the most dominant type of vibration problem found in machining operations. In the real part of the FRF, it is found strong relations to regenerative chatter, and thru analyzing turning operations theoretically, we see that there is a critical cutting depth  $a_{\text{lim}}$  differentiating stable and unstable behavior (Altintas 2012).  $a_{\text{lim}}$  is found by the formulation:

$$a_{\text{lim}} = \frac{-1}{2K_s \text{Re}(H(j\omega_c))} \quad (47)$$

Where:

- $k_s$  is the cutting force
- $\text{Re}(H(j\omega_c))$  is the real part of the FRF
  - $\omega_c$  is the chatter frequency

In regenerative chatter,  $\omega_c$  vibrates at the boring bar eigenfrequency or higher directly connected to the RPM of the workpiece. As seen in Eqn.47,  $a_{\text{lim}}$  becomes positive only by negative values of the real part of the FRF. Due to efficiency, as high cutting depth as possible while still maintaining a stable process is of high interest. Eqn.47 shows that  $a_{\text{lim, min}}$  must be at the maximized negative value of the FRF real part. In order to tune the TMD Sims 2007 showed that the maximized negative value of the FRF real part is at the optimal frequency:

$$\omega_{2, \text{opt}} = \sqrt{\frac{\mu + 2 + \sqrt{2\mu + \mu^2}}{2(1 + \mu)^2}} \omega_1 \quad (48)$$

In addition, he also found the damping ratio for a maximized negative value of the FRF real part is equal to the one for the minimized magnitude of FRF, Eqn.46

Eqn.45, 46 and 48 all assume  $c_1$  to be neglectable.

## 4.7 Constitutive Models for Rubber

Rubber materials are present in many applications for instance car tires, shock-absorbers, seals, and vibration dampers. Due to the increasing use of rubbers in the world of mechanical engineering, damping, and other applications, the need for good mathematical models to describe material behavior is high. Elastomers have complicated non-linear behavior, both viscoelastic behavior and hyperelastic behavior, they are incompressible and have very different behavior depending on the temperature. The nonlinear behavior of rubbers becomes prominent at large deformations, hysteresis, and viscoelasticity come into play at high strain rates. There are two main material model categories used to describe rubbers: Linear viscoelastic models, and hyperelastic models. Viscoelastic models are normally used at lower strains, and at higher phase-temps (above rubber plateau), and hyperelastic at larger, with a lower strain limit between the methods at stiffer materials. This chapter will describe the different categories and some of the specific material models in each category.

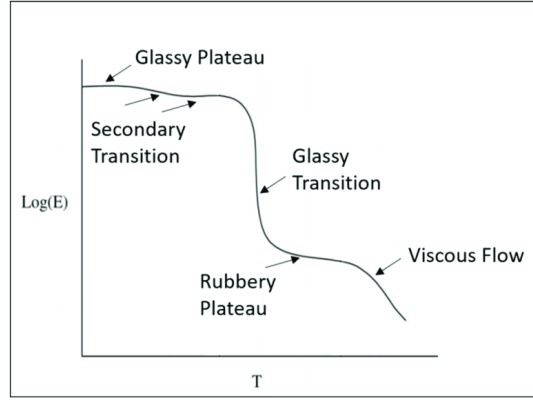


Figure 9: Rubber temperature shift

**Linear Viscoelastic models:** Elastomers have a shear modulus depending on the loading history and loading duration. We denote deformation:  $\gamma$  and stress state:  $\tau$ . It is seen that when elastomers are subjected to a constant deformation:  $\gamma_0$  over time, the stress decreases towards a limit:  $\tau_{lim}$ . This behavior is known as viscoelasticity. The linear viscoelastic models do not account for the nonlinear behavior at large deformations (Kraus et al. 2017).

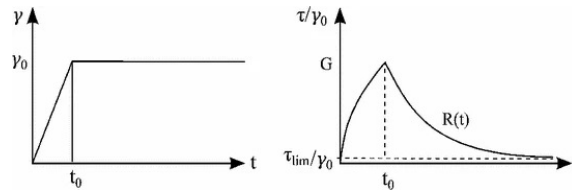


Figure 10: Viscoelasticity

Source: <https://link.springer.com/article/10.1007/s40940-017-0042-9/figures/1>

**Hyperelastic models** Hyperelastic material models are generally an extended isotropic linear elastic model that incorporates the nonlinear and large strain behavior when stress is introduced. Hyperelastic materials assume isotropic and incompressible qualities. Mathematical representations are often challenging due to their incompressible nature. A much used workaround is to apply a penalty method, which introduces a certain degree of compressibility to the strain energy density function. This penalty function essentially amends the strain energy function, rendering the material nearly incompressible rather than perfectly incompressible meaning that the bulk modulus is lower than infinity.

$$\kappa = \frac{E}{3(1 - 2\nu)} \quad (49)$$

Where:

- $\kappa$ : Is the bulk modulus
- $E$ : Is Young's modulus
- $\nu$ : Is the Poisson ratio

Hyperelastic material models are generally defined in terms of the Helmholtz free energy per unit volume, denoted as either  $\Psi(\mathbf{b})$  or  $\Psi(\mathbf{C})$ . This energy is dependent on the principal stretches  $\lambda_i$ , with  $i \in \{1, 2, 3\}$ .

---

The Neo-Hookean model is a basic hyperelastic framework that depends on two primary material constants: the shear modulus ( $\mu$ ) and the bulk modulus ( $\kappa$ ). The corresponding Helmholtz free energy function is represented in Eqn.50.

$$\Psi(I_1^*, J) = \frac{\mu}{2}(I_1^* - 3) + \frac{\kappa}{2}(J - 1)^2 \quad (50)$$

The Cauchy stresses for the standard experiments, assuming incompressibility of the material, can be calculated using Eqn.51 and 52.

$$\sigma_{\text{true,uniaxial}} = \mu \left( \lambda^2 - \frac{1}{\lambda} \right) \quad (51)$$

$$\sigma_{\text{true,biaxial}} = \mu \left( \lambda^2 - \frac{1}{\lambda^4} \right) \quad (52)$$

**Mooney-Rivlin** The Mooney-Rivlin hyperelastic model is an expansion of the Neo-Hookean material model and is defined by three material constants:  $C_{10}$ ,  $C_{01}$ , and the bulk modulus  $\kappa$ . In more detail,  $C_{10}$  and  $C_{01}$  are the coefficients of the first and second invariants of the right Cauchy-Green deformation tensor in the strain energy function. They essentially characterize the material's response to deformation, with  $C_{10}$  usually being associated with the material's resistance to shear, and  $C_{01}$  being associated with the material's resistance to volumetric changes.

It's important to note that these are empirical constants, meaning their values are determined from experiments and not from fundamental physical principles. As such, they can vary widely depending on the specific material being modeled.

The Helmholtz free energy function can be expressed as:

$$\Psi(I_1^*, I_2^*, J) = C_{10}(I_1^* - 3) + C_{01}(I_2^* - 3) + \frac{\kappa}{2}(J - 1)^2 \quad (53)$$

Assuming the material is incompressible, the Cauchy stresses for the standard experiments can be computed as:

$$\sigma_{\text{true, uniaxial}} = 2 \left( \frac{\lambda^2 - 1}{\lambda} \right) [C_{10} + C_{01}\lambda] \quad (54)$$

and

$$\sigma_{\text{true,biaxial}} = 2C_{10} \left( \frac{\lambda^2 - 1}{\lambda^4} \right) + 2C_{01} \left[ \frac{\lambda^4 - 1}{\lambda^2} \right]$$

Simulating rubber in FEM analysis:

The quality of finite elements employed for these computations greatly impacts the numerical stability, with higher-order elements generally providing more stability than lower-order ones. When using hyperelastic models for nonlinear studies, it's necessary to define constants directly or provide experimental data for internal computation. The load step and mesh should have careful consideration (Harish 2016).

---

## 5 Methodology

This thesis revolves around the subject of vibration-damping, and constitutive models for rubber materials in order to accurately describe real-world events thru simulations. In order to tune and validate the simulations and quantify them against real-world events, both simulations in Comsol Multiphysics and measurements from the lab at Sandvik Teeness have been developed and executed. They are ultimately giving the thesis data for quantifying goals and objectives, as well as providing both me and the reader a degree of insight into the ability of the simulation to represent physical structures like a vibration-dampened tool-holder. As viscous damping was excluded from the scope of this thesis, the lab experiments were all conducted with a TMD not containing any damping fluid. Thru this chapter of the thesis, I will provide the methods used in the development of my simulations in Comsol Multiphysics, the execution of the lab experiments, and how data has been treated in order to prepare for experimental validation and comparison. This chapter will also provide the reasoning behind some of my choices, with backing from the theory and literature study chapter.

### 5.1 Comsol Multiphysics Software

Comsol Multiphysics is a sophisticated computational tool utilizing the finite element method for solving and analyzing a wide field of physics and engineering areas, including but not limited to, structural mechanics, heat transfer, fluid dynamics, electromagnetics, and chemical engineering. It is a powerful tool for modeling and simulation of intricate systems and processes such as vibration-damped tool holders. As stated in its name, Comsol Multiphysics can deal with coupled-field issues that require simultaneous consideration of multiple physics, such as an interlinked electro-magnetic-thermal-structural analysis by creating multiphysics couplings in the software. Furthermore, Comsol Multiphysics post-processing instruments make it possible for the engineer to present data with a vast set of possible visual representations, enabling thorough examination of the resulting data sets.

The software enables engineers to conduct complex simulations in order to increase the understanding of real-world systems, their behavior, and key system parameters. Comsol offers the potential to optimize the design of engineering components and entire systems thru topology, parameter, and other optimization tools (Comsol 2023e). Its applications span a wide spectrum of fields including automotive, aerospace, electronics, energy, and medical devices.

For the purpose of this thesis, Comsol Multiphysics was chosen due to its robust capabilities in simulating vibrations and coupled-field phenomena. These abilities proved particularly crucial in the development and refining of the simulation models. Especially useful on the path was the possibility of making a lumped-mechanics-beam-physics coupled mechanics simulation. These functionalities along with the wish for a deeper investigation of Comsol as a multiphysics and FEM analysis software led to the preference of Comsol over Abaqus, having prior experience with the latter, particularly in static strength simulations with contact interaction between parts.

For the basics of how the Comsol Multiphysics environment is set up, and how to navigate and set up simulations I refer to my autumn semester thesis. Here you can also find possible fall pits and tips that are based on my personal experience with the software.

---

## 5.2 Modeling and Simulation of Vibration Damped Tool Holders

The journey to achieving full 3D simulations of a two-mass solid mechanics system, including linear elastic and hyperelastic material models, has been a thorough and comprehensive process. It has involved countless simulations and hours invested in self-study and in-depth research towards Comsol simulations and the field of vibrations which was totally new to me. The project's progress has been staccato in its form due to its "learning by doing" nature. Having to gain more insight and knowledge in order to troubleshoot and develop my Comsol simulations. Various forum threads, as well as direct contact with Comsol support also played an important role in overcoming obstacles encountered throughout both the autumn semester thesis and this master's thesis.

The method of taking small steps in the development of increasingly complex simulations has been a governing factor for success. Giving motivation by creating a more continuous although staccato progress, with many smaller milestones. Taking small steps thru the autumn also helped to adjust and set a realistic scope for the thesis. It was thru my initial simulations and knowledge-building in the field of fluid simulations that the decision of excluding viscous damping from the scope of the thesis was made. A decision I deem wise in retrospect.

### 5.2.1 A general walk-thru of the final simulations

Two final solid mechanic simulations will be presented in this thesis. One simulation model contains a rubber-steel-rubber tube assembly, modeling a TMD without oil, and one with the TMD assembly model within a boring bar. In both simulations, the rubber parts in the TMD are modeled using the hyperelastic: Neo-Hookean incompressible material model, and the rest of the components are modeled with Linear elastic isotropic material models. See the simplified machined drawing(appendix) in order to see the parts dimensions and corresponding materials.

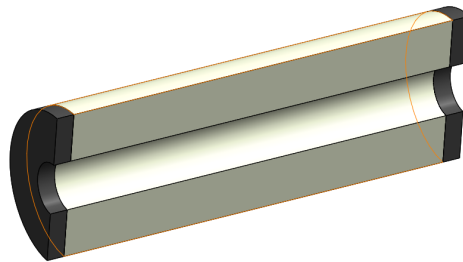


Figure 11: Simulation assembly model of a TMD without viscous damping(section view)

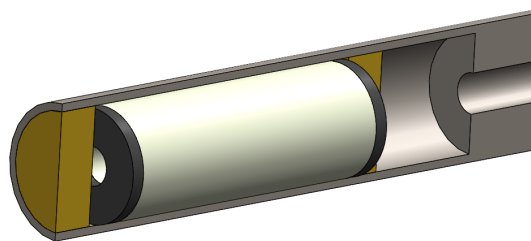


Figure 12: Boring bar(section view) simulation assembly model with TMD

In order to both reduce the computational load as well as to continue the methodology of increasing the complexity of the simulations at a steady pace, it was decided to conduct a simulation only containing the TMD without damper fluid Fig.11 before moving on to the full assembly simulation model Fig.12.

---

## 5.2.2 Simplified TMD Comsol Simulation

### General:

A central objective for the development phase of the simulation was to include a hyperelastic material model for the rubber materials. The reasoning behind this was to be able of comparing different material models, such as isotropic linear elastic towards hyperelastic Neo-Hookean. The hyperelastic model Neo-Hookean was chosen due to the assumption of operating temperature well below the transition phase to the viscoelastic behavior of the rubber springs. A governing factor was also the simplicity of the Neo-Hookean, as no material-specific tests were done on the rubber materials to find parameter values. With the Neo-Hookean material model, calculating the spring stiffness coefficient based on lab data leads to the start point of the bulk modulus parameter value before tuning. As the strains are kept relatively low in the simulations, this essentially means that we are using an isotropic linear elastic material model (not entering the hyperelastic behavior at large strains), this is described in the theory and literature study Chap.4.7. The hypothesis was tested and confirmed by testing over a variation of force magnitudes seen in Table 8. In order to make the thesis results more redundant, the simplified TMD simulations have been performed at two different evaluation points giving two different result outputs: 1st evaluation point at the mid-length of the damper mass capturing only eigenmode 1, and 2nd: evaluation point at the end of the damper mass capturing both first and second eigenmode. This was also done in the lab, by placing the accelerometer at the two different evaluation points.

### Materials:

- Tungsten
  - Material model: Linear elastic, isotropic
  - Young's modulus: 360 [Gpa]
  - Poisson's ratio: 0.28
  - Density: 17800 [Kg/m<sup>3</sup>]
- Rubber
  - Material model: Hyperelastic, Neo-Hookean
  - Damping: Isotropic structural loss factor: 0.08
  - Compressibility: Incompressible
  - 2nd Lamé parameter( $\mu$ ): 1.75[Mpa]
  - Density: 1100[Kg/m<sup>3</sup>]

### Geometry:

The assembly of the parts making the simplified simulation model of the TMD is made in the CAD program SolidWorks, and imported into Comsol by the use of the import function for 3D CAD files. When importing geometry with touching faces, they are joined by bonded contact meaning that the surfaces are completely coupled but can be deformed. The Damper mass was also partitioned on the mid-length of the axle to create boundaries to both set the load on and evaluation point for the resulting output of the simulation.

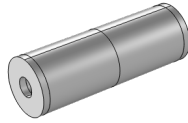


Figure 13: Comsol view of imported and partitioned geometry, TMD assembly

**Physics:**

For the simulation, only Structural Mechanics physics was used.

**Load:**

A point load is used to perform a convergence study on the mesh based on a stationary study, as well as to conduct an evaluation of the linearity of the system. Two attack points were set in order to do a proper evaluation of the damper 1st. and 2nd. eigenfrequency mode shapes and corresponding frequency response, the two load attack points are run in separate simulation steps.

- Point Load: 0.1, 1, 10[N], Used for the stationary study.
- Point Load Harmonic Perturbation: 1[N], Used for the Frequency domain studies
  - attack point: center of damper mass length
  - attack point: end of damper mass length

**Damping:**

The rubber elements are damped by the use of an isotropic loss factor that describes the ratio of energy dissipation per oscillation. This is a way to replicate solid damping in the material due to energy dissipation. When using the Neo-Hookean hyperelastic material model, the loss information is given as a multiplier in strain energy density, in the second Piola-Kirchhoff stress,  $S$ . (Comsol 2023d). The value of the isotropic loss factor has been selected in order to give a satisfactory according to the lab results. Changing the damping affects the amplitude and rate of change in magnitude greatly. Higher value, lower amplitude, and lower rate of change in magnitude.

- Rubber springs: Isotropic structural loss factor: 0.08

**Boundary conditions:**

The outer surfaces of the simplified TMD assembly are fully constrained in all translational and rotational directions. Done by a Fixed constraint.

**Meshing:**

The meshing is done by a convergence study on the stationary deflection study.

- Element type: Free Tetrahedral
- Element size: Normal
  - Max size: 9.8mm
  - Min size: 1.76mm

- 
- Max growth rate: 1.5
  - Displacement field: Quadratic serendipity
    - Les nodes than Lagrange element but still good results and less computational load

**Study (Stationary: Static Deflection):**

The Stationary study was conducted in order to check the linearity of the system. The study was run with the three point loads given above.

**Study (Eigenfrequency):**

The Eigenfrequency study excludes all loads and damping is deactivated for the study, giving the undamped eigenfrequencies.

**Study (Frequency Domain, Modal: Harmonic Vibration):**

Includes an initial step, eigenfrequency study, creating the basis for the frequency domain, and modal analysis. The modal analysis runs parameter stepping in the frequency domain, giving the frequency response as output. The modal solver reduces the model by using the precalculated eigenfrequencies to find eigenpairs, constructing a basis of dominant eigenvectors for the dominant frequencies found. The method is highly efficient in terms of computational speed due to the way of solving the underlying equation system by approximation of the parametric coefficients together with the dominant eigenvectors (few) (Comsol 2023c).

For study step 1: eigenfrequency study, all damping is disabled.

To represent the two different configurations: Center(translation) and Side(translation and rotation) there exist two different studies, with the corresponding load activated and all other loads deactivated. The studies also have different evaluation points to capture the movement. The evaluation points are at the same boundary point as the attack point of the load

In the result section of the simulation, two 3D evaluation points are selected for creating the corresponding 1D plot groups. The plot data is plotted as "solid.disp rms", which gives the root mean square of the result values. The RMS function was chosen to account for oscillating values between positive and negative values as the values are squared removing the negative sign and filtering extreme variations by the root mean value.

All results from the study have then been added to an export group in Comsol and exported as .txt files. The data is treated together with the results from the lab in a self-developed Python script for both single representation and different types of comparison plots.

For the parameter stepping in both studies of the simulation, the following frequency steps in Hz were decided based on the results of the Eigenfrequency study, (lower limit, step size, upper limit):

- Frequencies: range(0,2,100), range(100,0.05,150), range(150,2,220), range(220,0.05,300), range(300,2,350)

### 5.2.3 Simplified Boring Bar with TMD Comsol Simulation

**General:**

As the simulation with the simplified TMD model was up and running in a satisfactory manner, the full assembly simulation was next in line. The main objectives for the development of the simulation included creating correct relations between selected parts in order for the model to function similarly to real-world events. The simulation in itself is built on many of the same blocks as the simplified TMD simulation. The three new components, with the one "boring bar" and the two "TMD Restrainer" parts, structural steel, are also added to the simulation, following the isotropic linear elastic material model. The parts and belonging material can be seen in the appendix. In order to make the thesis results more redundant, the full assembly simulations have been run at three different free lengths of the boring bar. 10xD: 400mm, 11xD: 440mm, and 12xD: 480mm, according to the lab experiments



---

**Material:**

- Tungsten
  - Material model: Linear elastic, isotropic
  - Young's modulus: 360 [Gpa]
  - Poisson's ratio: 0.28
  - Density: 17800 [Kg/m<sup>3</sup>]
- Rubber
  - Material model: Hyperelastic, Neo-Hookean
  - Damping: Isotropic structural loss factor: 0.08
  - Compressibility: Incompressible
  - 2nd Lamé parameter( $\mu$ ): 1.75[Mpa]
  - Density: 1100[Kg/m<sup>3</sup>]
- Structural Steel
  - Young's modulus: 200[GPa]
  - Poisson's ratio: 0.3
  - Density: 7850 [Kg/m<sup>3</sup>]

**Geometry:**

The assembly of the parts making the simplified boring bar and TMD is made in the CAD program SolidWorks, and imported into Comsol by the use of the import function for 3D CAD files. When importing geometry with touching faces, they are joined by bonded contact meaning that the surfaces are completely coupled but can be deformed. The boring bar was also partitioned at three places corresponding to the free lengths 400mm, 440mm, and 480mm in order to create relevant boundary conditions.



Figure 14: Comsol view of imported and partitioned geometry, Boring bar assembly

**Physics:**

For the simulation, only Structural Mechanics physics was used.

**Load:**

The study only includes one harmonic perturbation point load located on the tip of the free end. This load is used on all the different length variations of the free length.

- Point Load Harmonic Perturbation: 1 [N], used for the frequency domain studies.

---

**Damping:**

The Rubber springs are damped by the same isotropic loss factor as found in the study of the simplified TMD in order of conducting an analysis with constant parameter values to make a solid relation to the lab experiments. The boring bar is damped with Rayleigh damping as done in the autumn semester thesis. Rayleigh damping model is similar to friction loss and is not frequency dependent, it was found to provide a stable model with satisfactory results in previous studies conducted in my autumn semester thesis, and the same values have been used in the simulations presented in this master's thesis.

- Rubber springs: Isotropic structural loss factor: 0.08
- Boring bar: Rayleigh damping
  - Mass damping parameter ( $\alpha_{dM}$ ): 5.36 [1/S]
  - Stiffness damping parameter ( $\beta_{dK}$ ): 7.46e-5 [s]

**Boundary conditions:**

Depending on the study three different boundary conditions are active for each study. the boring bar is locked with a fixed constraint at the domains created by the partitioning. resulting in the free lengths: 400mm, 440mm, and 480mm

**Meshing:**

The meshing is the same as found by the convergence study on the stationary deflection study done in the simplified TMD simulation. Verification of small variances on refining was done in order to ensure the convergence study validity. This proved the hypothesis that the TMD was the most demanding subassembly in terms of mesh size, therefore not needing further refining.

- Element type: Free Tetrahedral
- Element size: Normal
  - Max size: 9.8mm
  - Min size: 1.76mm
  - Max growth rate: 1.5
- Displacement field: Quadratic serendipity
  - Less nodes than Lagrange element but still good results and less computational load

**Study (Eigenfrequency):**

The Eigenfrequency study excludes all loads, and damping is deactivated for the studies, giving the undamped eigenfrequencies. Three Eigenfrequency studies are conducted, one for each variation of the free length. The eigenfrequencies found in the studies are the basis for the frequency ranges chosen for the frequency domain, modal studies.

**Study (Frequency Domain, Modal, Harmonic Vibration):**

Three equal frequency domain, modal studies are conducted, one for each variation of the free length. The 1st. step in the studies is an eigenfrequency study, creating the basis for the frequency domain, modal analysis. The modal analysis runs parameter stepping in the frequency domain, giving the frequency response as output. The modal solver reduces the model by using the pre-calculated eigenfrequencies to find eigenpairs, constructing a set of dominant eigenvectors for the dominant frequencies found. The method is highly efficient in terms of computational speed due to the way of solving the underlying equation system by approximation of the parametric coefficients together with the dominant eigenvectors (few).

In the eigenfrequency study step of the modal analysis, all damping is deactivated to avoid problems occurring in the modal solver with the imaginary part included by damping.

---

In the result section three separate 3D evaluation points are created at the same domain point (at the free end) and assigned data from each of the different free-length solutions. A corresponding 1D plot group is made for each of the 3D evaluation points. The plot data is plotted as "solid.disp rms", which gives the root mean square of the result values. The RMS function was chosen to account for oscillating values between positive and negative values as the values are squared, removing the negative sign and filtering extreme variations by the root mean value.

All results from the study have then been added to the export group in Comsol and exported as .txt files. The data is treated together with the results from the Lab in a self-developed Python script for both single representation and different types of comparison plots.

For the parameter stepping in the studies the following frequency ranges in Hz was decided on the background of the Eigenfrequency studies, (lower limit, step size, upper limit):

- Harmonic forced vibration, 400mm: range(0,2,50), range(50,0.01,150), range(150,2,240), range(240,0.01,340), range(340,2,1200)
- Harmonic forced vibration, 440mm: range(0,2,50), range(50,0.01,150), range(150,2,200), range(200,0.01,300), range(340,2,1200)
- Harmonic forced vibration, 480mm: range(0,2,50), range(50,0.01,125), range(125,2,175), range(175,0.01,300), range(300,2,1200)

### 5.3 Lab Experiments at Sandvik Teeness

A central part of the thesis and the basis for adjusting the rubber material model in order to get results similar to the real-world behavior of the TMD and boring bar is the data from Lab experiments conducted by Dan Östling at Sandvik Teeness. The fact that Dan and Sandvik Teeness supported me with the testing, and me being present at the Lab while testing, was an important factor of motivation throughout the thesis work.

The tests performed were impulse response tests. A force impulse was given to the test structure, with a sensor measuring the impulse (force/time), and an accelerometer attached to the oscillating structure by a magnet. The measurements were tracked in the time domain and an FFT: Fast Fourier Transform gave the resulting data in the frequency domain. Each experiment consisted of 8 impacts and then a mean of these was calculated as the resulting data.



Figure 15: Impact Hammer

For redundancy and to capture the eigenmodes properly, two test setups were conducted on the TMD without damping fluid.

1. Impulse impact and measurement on the middle of the damper mass length
2. Impulse impact and measurement on the end of the damper mass length

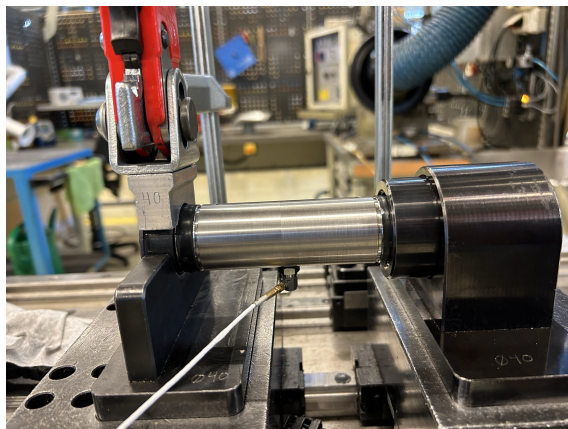


Figure 16: Setup in test bench: TMD without oil and accelerometer under mid-length

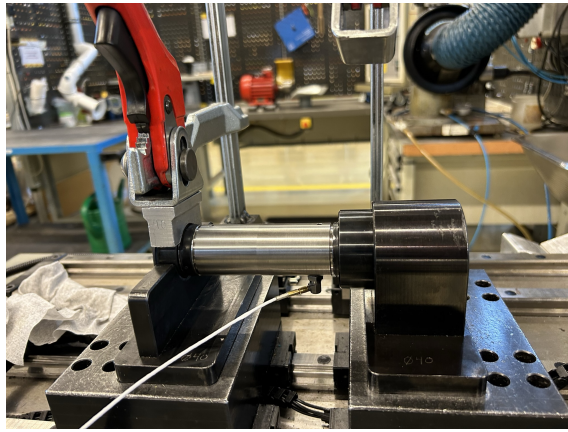


Figure 17: Setup in test bench: TMD without oil and accelerometer under end of damper mass

Three test setups were conducted with the TMD installed in the boring bar, still with no damping fluid. The accelerometer was placed at the free end of the bar through all three setups.

1. 10xD: 400mm free length
2. 11xD: 440mm free length
3. 12xD: 480mm free length

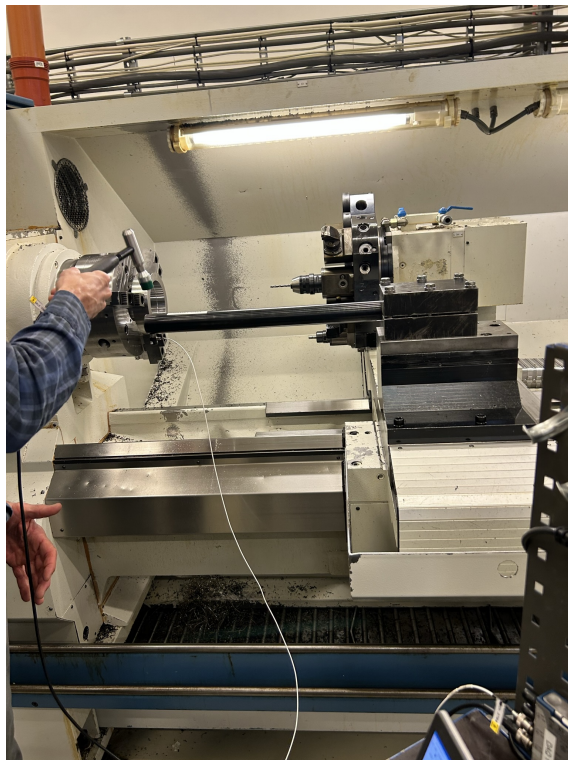


Figure 18: Setup in the lathe for impulse test of the boring bar with TMD (without damper fluid). An accelerometer at the tip of the free end

---

## 5.4 Experimental Validation

In order to set up the simulations for experimental validation, the rubber model needed to be tuned. As the damper mass was given from Sandvik to be 1.19kg and the first mode eigenfrequency was found in the lab results to be 120Hz. Initial parameter values could be calculated:

$$k_{tot} = (F_n \cdot 2\pi)^2 \cdot m$$

$$k_{tot} = (120 \text{ Hz} \cdot 2\pi)^2 \cdot 1.19 \text{ kg}$$

$$k_{tot} = 676502 \text{ N/m}$$

$$G = \frac{k}{A} \cdot d$$

$$G = \frac{676502 \text{ N/m}}{\left(\frac{\pi}{4}(33.5^2 - 11.5^2)\right) \cdot 10^{-6} \text{ m}^2} \cdot 2 \cdot (4) \cdot 10^{-3} \text{ m}$$

$$G = 2.568 \text{ MPa}$$

Where:

- $k$  is spring constant [N/m]
- $F_n$  is the eigenfrequency [Hz]
- $m$  is mass [kg]
- $A$  is area [m<sup>2</sup>]
- $d$  is thickness [m]
- $G$  is the shear modulus [Pa]

### Initial Values

Incompressible rubber material gives Poisson's ratio = 0.5

Isotropic structural loss factor(recommended by Sandvik representant) =0.06

2nd. Lamé parameter:  $\mu = G = 2.568 \text{ MPa}$

In order to perform the tuning it is of interest to use results with as few uncertainties as possible. Due to this, the TMD translational case will be used as the case for parameter tuning, and the resulting parameter values found will be used for all other simulation cases, to replicate the real world as the parameters stay the same in all the lab experiments. The first objective for the tuning is to match the frequency of the peak value in the lab to the one in the simulation. This will be done by increasing(higher eigenfrequency) or decreasing(lower eigenfrequency) the 2nd. Lamé parameter dependent on whether or not the simulation peak frequency is lower(increase) or higher(decrease) than the lab eigenfrequency. After the Lamé parameter is found, the shape of the curve is the next objective. The shape is to be adjusted by steady steps up(slower rate of change in frequency response) or down(faster rate of change in frequency response) in the isotropic structural loss factor. The goal is to adjust the curve so that the fit after applying a scalar value to the simulation curve, the two curves of the lab and simulation will fit as well as possible. For the damping factor, a visual approximation is considered good enough.

The results from the lab, simulation, and comparison of these have all been plotted by the use of my Python script, this was done to avoid screenshots from Comsol and to enable equal visual representation, and most importantly, the ability to put data sets from both lab and simulation in the same plot and perform magnitude adjustment, ultimately providing an informative visual representation of the results. The simulation and Lab results were compared in the frequency response with the magnitude plotted on the y-axis (mm for the simulations and mm/N for the lab) and the frequencies plotted on the x-axis in Hz. Due to the lab results represented as compliance [mm/N] all simulations were run with 1N force magnitude to remove the need for any post-calculation of magnitude for correct comparison between lab and simulation results.

---

The Lab results were handed to me with values of the real and imaginary part of the FRF as acceleration:  $[m/s^2/N]$ . To convert the values into magnitude in the form of compliance:  $[m/N]$ , we first divide both parts with the angular frequency:  $(2 * \pi * f)^2$ .

Then we square the imaginary and real parts, add them together, and apply the root:  $\sqrt{(\text{Re})^2 + (\text{Im})^2}$

The presentation of the results from the simulation and lab is structured by presenting case by case.

1. TMD without oil
  - (a) Results of parameter tuning
  - (b) Eigenfrequencies and Eigenmodes
  - (c) Lab and simulation frequency response, translation
  - (d) Lab and simulation frequency response, translation, with amplitude correction on the simulation result.
  - (e) Lab and simulation frequency response, translation and rotation
  - (f) Lab and simulation frequency response, translation and rotation, with amplitude correction on the simulation result.
2. Boring bar with TMD(without damping fluid)
  - (a) Comparison of the three free-length variations
  - (b) Free length 10xD: 400mm
    - i. Eigenfrequency and Eigenmodes
    - ii. Lab and simulation frequency response
    - iii. Lab and simulation frequency response, with amplitude correction on the simulation result.
  - (c) Free length 11xD: 440mm
    - i. Eigenfrequency and eigenmodes
    - ii. Lab and simulation frequency response
    - iii. Lab and simulation frequency response, with amplitude correction on the simulation result.
  - (d) Free length 12xD: 480mm
    - i. Eigenfrequency and Eigenmodes
    - ii. Lab and simulation frequency response
    - iii. Lab and simulation frequency response, with amplitude correction on the simulation result.

The plots presenting the simulation and lab results are the basis of the experimental validation, and the peak values in the different cases will give an indication of the ability of the Comsol simulations to estimate the frequency and amplitude values of the real-world system eigenmodes. Eigenfrequencies and mode shapes are dependent on the geometry of the system, mass distribution, and stiffness properties, but the amplitude is dependent on factors like damping, boundary conditions, and specific excitation. Therefore, it is likely to be a larger deviation in the amplitude than in the frequency of the peaks. Therefore a scaling shall be performed on the simulation results, based on the first eigenmode amplitude. For the lab and simulation results on the simplified TMD assembly cases, the scaling is to be done based on the TMD translation case and applied to both cases due to the first eigenmode should be close to equal for both cases. Each of the varying free-length cases is to be scaled individually. In order to quantify the agreement between the lab and simulation peak values(frequency, and magnitude), the error of the simulation peak values shall be calculated against the lab peak values. Error estimations of the peaks in the amplitude-scaled simulation curves shall also be included to give insight into whether or not this reduces or increase the overall error of each case.

---

## 6 Simulation and Lab Results

This section will present all relevant results gained thru the thesis research, both lab and simulation data, as well as comparisons of the two. Emphasis has been put on providing informative and clear visualizations with a strong connection to the thesis goals and objectives. The results presented will all be subject to a discussion where I will present my evaluations and thoughts on both the results and the validity of the results.

### 6.1 TMD without oil

In order to perform tuning of the relevant rubber material parameters in my simulations, lab experiments had to be carried out to collect data from real-world behavior. Testing on the assembly with the least elements interfering with the eigenfrequencies of the system was of high interest, to decrease the complexity and minimize uncertainty. The testing on only a TMD assembly without oil was highly beneficial for the parameter tuning. The TMD translation case was used for tuning, and the parameter value of the second Lamé parameter was decreased by steady steps until the eigenfrequency of the TMD translation simulation and lab results were within the objective value of 5%. The isotropic structural loss factor was increased from its initial value of 0.06 and locked at 0.08. Even though this resulted in different amplitudes between the lab and simulation results the goal was to get a similar curve after magnitude correction. This was done by adjusting the simulation results by a scalar = (Lab peak magnitude) / (Simulation peak magnitude). The parameter value was accepted upon visual evaluation, not by numerical methods.

After a great number of iterations with decreasing step size, the final parameters included in the Neo-Hookean hyperelastic material model used to model the rubber elements in my simulations were locked at the following values:

- 2nd. Lamé parameter ( $\mu$ ) : 1.75Mpa
- Isotropic loss factor: 0.08

Giving the following results in the simplified TMD simulation:

<b>Eigenmode</b>	<b>Eigenfrequency [Hz]</b>
1	119
2	240

Table 2: Simulated Undamped Eigenfrequencies (Simplified TMD simulation)



The mode shapes from the frequency domain modal simulation with their respective frequency are seen in the figure below:



(a) Simplified TMD, Modeshape at 119Hz

(b) Simplified TMD, Modeshape at 240Hz

Figure 19: Simplified TMD, Modeshapes

**First Mode (Translational Mode):** The first mode of vibration for the TMD is similar to the first mode of a simply supported beam. It represents a half-sine wave along the length of the assembly. In this mode, the entire damping mass moves up and down, essentially translating parallel to its steady state position. All of the deformations occur in the rubber springs, as there is very little force acting on the very stiff damping mass. This mode, as seen in this simulation usually has the lowest frequency of all the vibrational modes and is often referred to as the fundamental or primary mode of vibration.

**Second Mode (Rotational or Bending Mode):** The second mode of vibration represents a full sine wave along the length of the TMD, similar to the second mode of a simply supported beam. In this mode, the damping mass oscillates with a nodal point at the center of the body. The nodal point remains stationary while the ends of the body move in opposite directions. This results in a bending or rotational motion around an axis thru the nodal point in the damping mass body's radial direction.

Comparison between lab and simulation, Translational movement(mode 1):

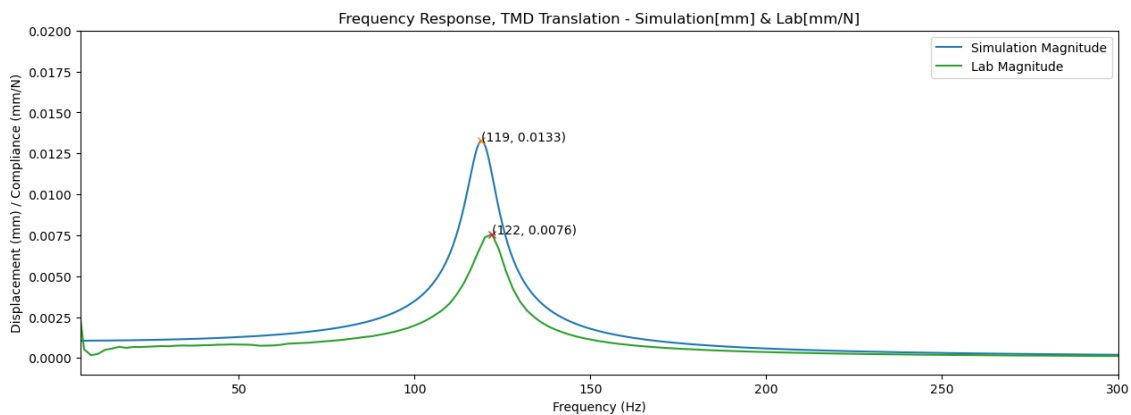


Figure 20: Comparison between Lab and Simulation, TMD: Translation

Adjusting for the amplitude difference gives the following result:

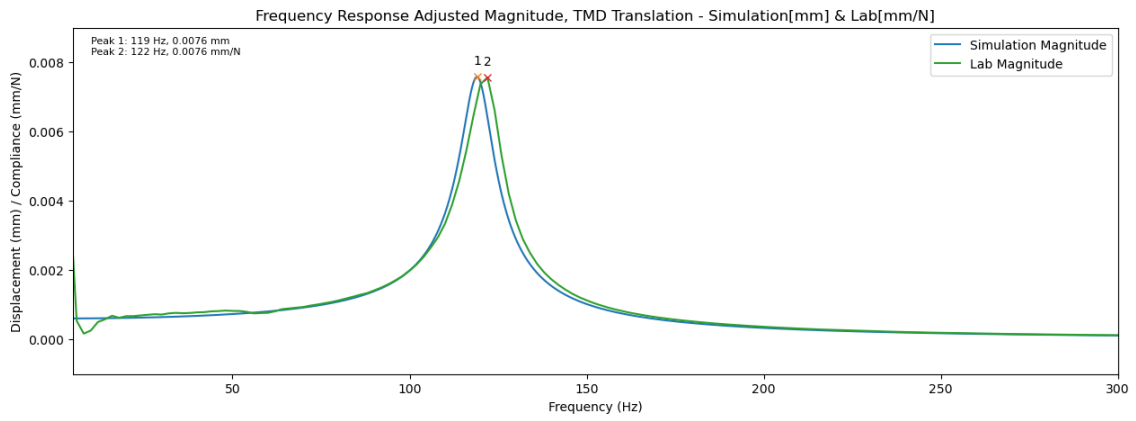


Figure 21: Comparison between Lab and Simulation, Simplified TMD translation, Corrected Simulation Magnitude based on first mode peak values(Scalar= 0.571)

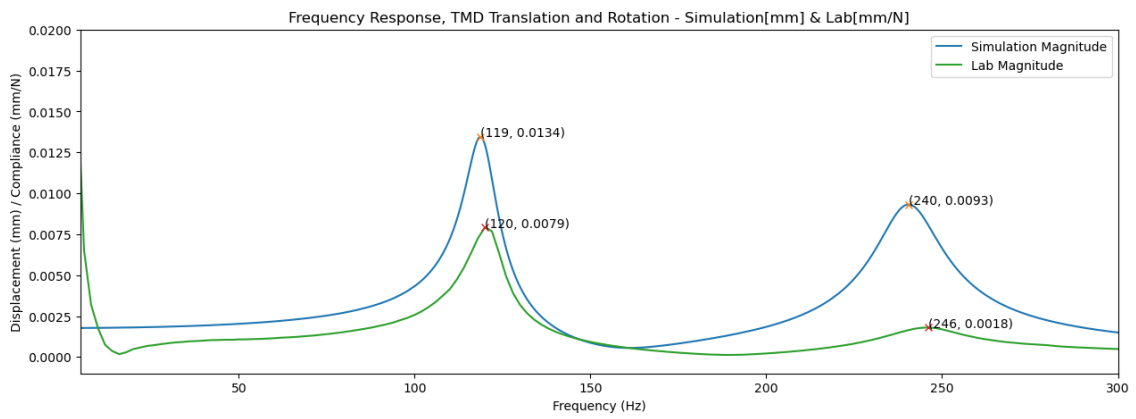


Figure 22: Comparison between Lab and Simulation, TMD: Translation and Rotation

The same scalar adjustment as in the pure translation case gives the following result:

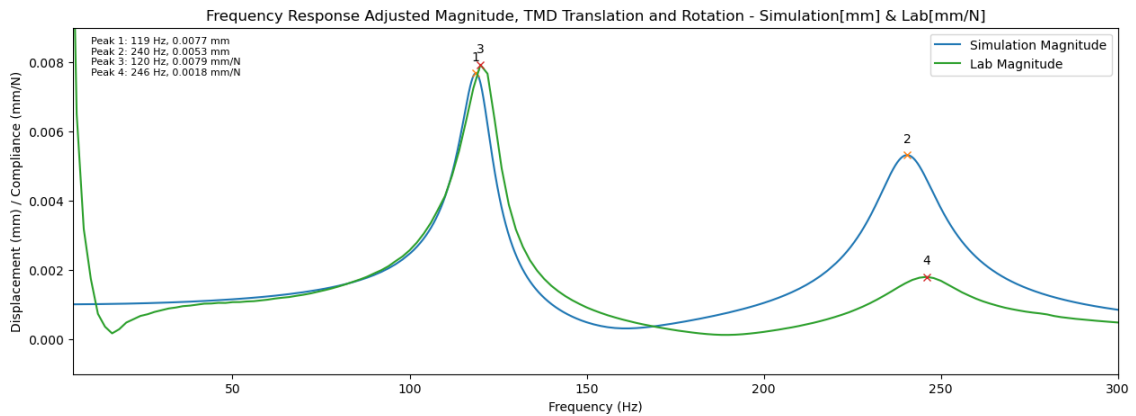


Figure 23: Comparison between Lab and Simulation, Simplified TMD translation and rotation, Corrected Simulation Magnitude based on first mode peak values(Scalar= 0.571)

---

## 6.2 Boring bar with TMD(without damping fluid)

After tuning the material model for the rubber elements, all parameters belonging to the TMD assembly were set and re-used in the full-assembly simulation. As the model increases in size, new uncertainties are added, such as the solid damping values of the boring bar. This chapter will present the simulation results of three configurations of the overhang(Free length). The chapter starts with a picture containing the lab result's frequency response curves of the three variations. Following, are the results of each and one of the three free-length variations in its own section.

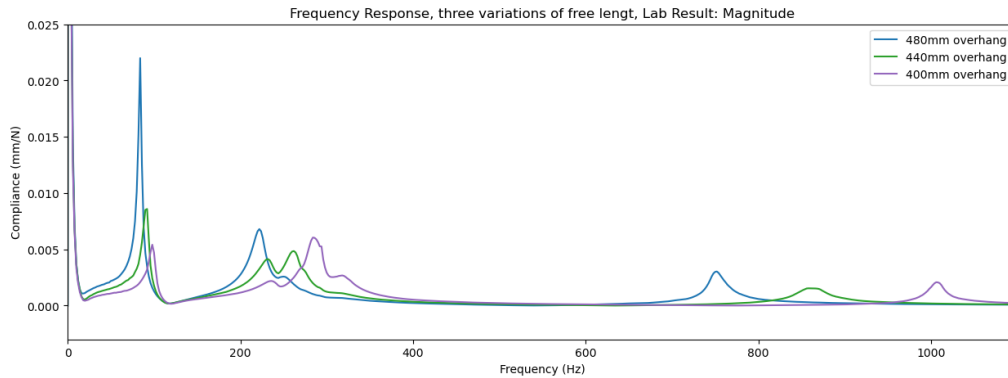


Figure 24: Lab: Frequency Response Function, Comparison of varying free length

The peaks in the frequency range: 700Hz-1100Hz are not considered further in the result section due to none of the simulations showing any peaks in this range. Therefore the frequencies at this high Hz are removed in order to provide a finer resolution of the impulse response curve ranges found in both simulation and lab results. This will be further commented on in the discussion section Chap.7.3.

### 6.2.1 Free Length 10xD: 400mm

Eigenmode	Eigenfrequency [Hz]
1	96
2	232
3	308

Table 3: Simulated Undamped Eigenfrequencies (Simplified Boring Bar, 400 mm)

The mode shapes from the frequency domain modal simulation with their respective frequency are seen in the figure below:



(a) Simplified Boring bar with TMD, Modeshape at 96Hz      (b) Simplified Boring bar with TMD, Modeshape at 232Hz      (c) Simplified Boring bar with TMD, Modeshape at 308Hz

Figure 25: Simplified Boring bar with TMD, 400mm, Undamped Modeshapes

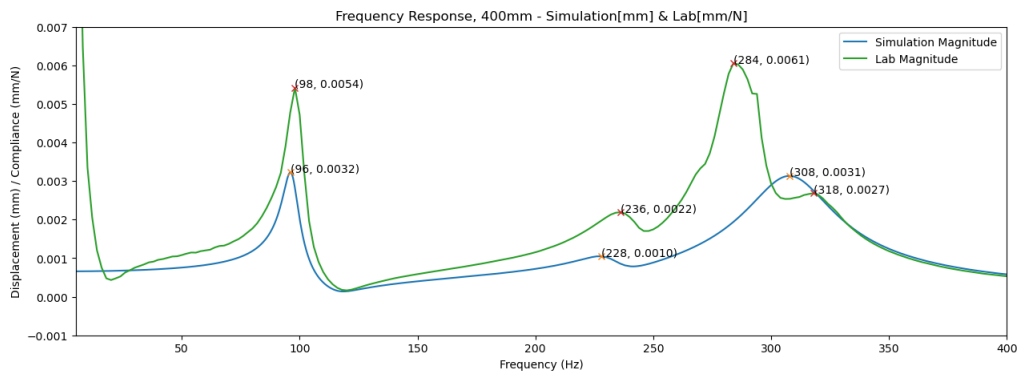


Figure 26: Comparison between Lab and Simulation, Free Length: 400 mm

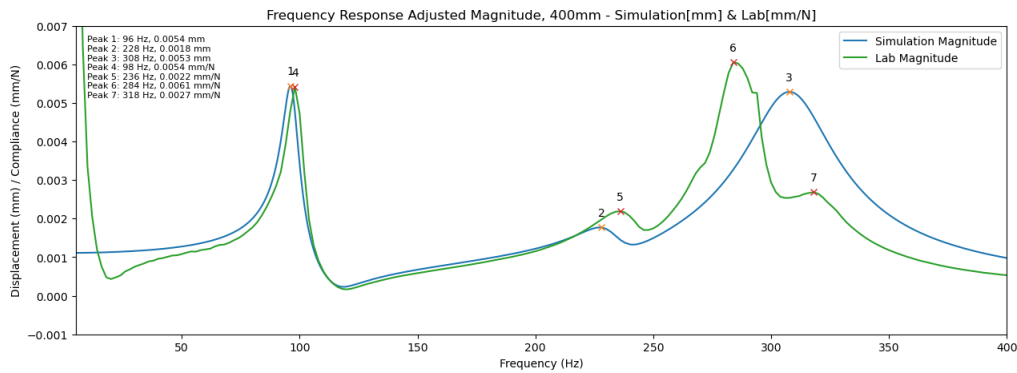


Figure 27: Comparison between Lab and Simulation, Free Length: 400mm, Corrected Simulation Magnitude based on first mode peak values(Scalar= 1.688)

## 6.2.2 Free Length 11xD: 440 mm

Eigenmode	Eigenfrequency [Hz]
1	91
2	230
3	271

Table 4: Simulated Undamped Eigenfrequencies (Simplified Boring Bar, 440 mm)

The mode shapes from the frequency domain modal simulation with their respective frequency are seen in the figure below:



(a) Simplified Boring bar with TMD, Modeshape at 91Hz

(b) Simplified Boring bar with TMD, Modeshape at 230Hz

(c) Simplified Boring bar with TMD, Modeshape at 271Hz

Figure 28: Simplified Boring bar with TMD, 440mm, Undamped Modeshapes

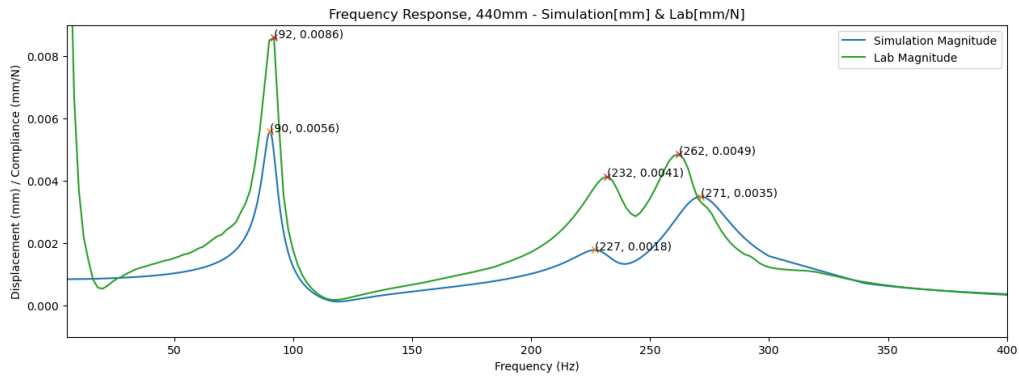


Figure 29: Comparison between Lab and Simulation, Free Length: 440mm

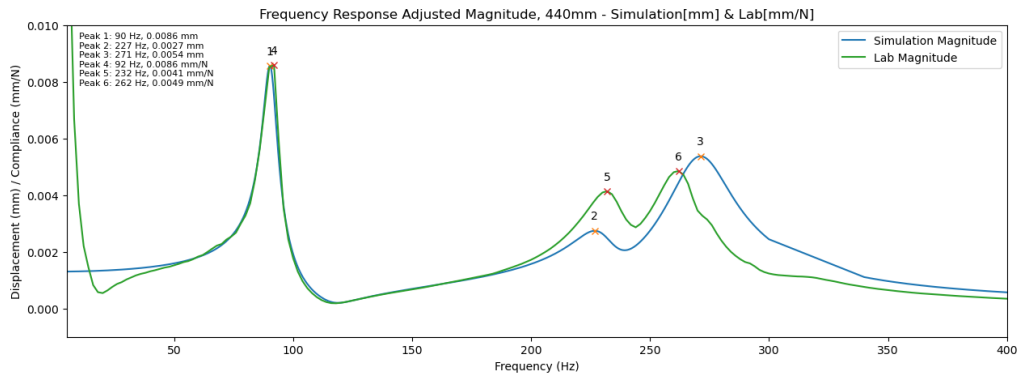


Figure 30: Comparison between Lab and Simulation, Free Length: 440mm, Corrected Simulation Magnitude based on first mode peak values(Scalar= 1.536)

### 6.2.3 Free Length 12xD: 480 mm

Eigenmode	Eigenfrequency [Hz]
1	84
2	224
3	247

Table 5: Simulated Undamped Eigenfrequencies (Simplified Boring Bar, 480 mm)

The mode shapes from the frequency domain modal simulation with their respective frequency are seen in the figure below:



(a) Simplified Boring bar with TMD, Modeshape at 84Hz

(b) Simplified Boring bar with TMD, Modeshape at 224Hz

(c) Simplified Boring bar with TMD, Modeshape at 247Hz

Figure 31: Simplified Boring bar with TMD, 480mm, Undamped Modeshapes

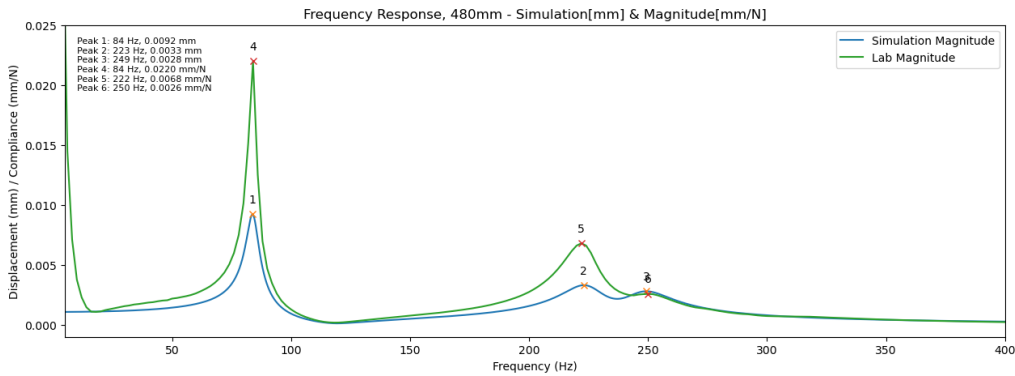


Figure 32: Comparison between Lab and Simulation, Free Length: 480mm

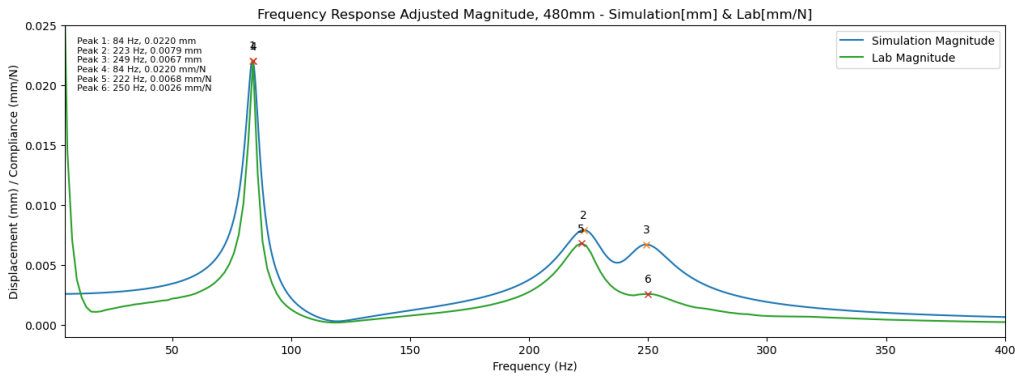


Figure 33: Comparison between Lab and Simulation, Free Length: 480mm, Corrected Simulation Magnitude based on first mode peak values(Scalar= 2.391)

---

#### 6.2.4 Comparison of simulations and lab results based on peak values

The peaks in the frequency response curves show the eigenfrequencies of the system. The taller the peaks are, the more dominant the mode is considered to be. The peak values are of high interest when it comes to considering the stability of a system and is used in the tuning method of the minimized magnitude of FRF Chap.4.6. We, therefore, want to look at the relation between Lab and simulation peak values(frequency, magnitude). This can give an indication of the performance to identify the frequencies at which the system can become unstable due to resonance, and the magnitudes will be of high interest when it comes to tuning the system for specific behavior and resistance against selected types of vibration.

For the simulated peak values(frequencies[Hz], and magnitude[mm]) the error is calculated against the lab results.

$$\text{Simulation error} = \frac{(\text{Simulated Value} - \text{Lab Value})}{\text{Lab Value}} \cdot 100\%$$

Case	Lab Freq.(Hz)	Sim. Freq.(Hz)	Sim. error(%)
TMD Translation and Rotation	120	119	-1%
	246	240	-2%
400mm *	98	96	-2%
	238	228	-3%
	284*	308*	8%*
	318	308	-3%
440mm	92	90	-2%
	232	227	-2%
	262	271	-3%
480mm	84	84	0%
	222	223	0%
	250	249	0%

Table 6: Comparison of lab and simulation peaks(Frequency)

\*Uncertain lab result, further elaborated in Chap.7.3

Case	Lab Disp.[mm/N]	Sim. Disp. at1N [mm]	Sim. error %
TMD Translation and rotation	0.0079	0.0134	70%
	0.0018	0.0093	416%
TMD Translation and rotation Scaled amplitude	0.0079	0.0077	-3%
	0.0018	0.0053	194%
400mm *	0.0054	0.0032	-41%
	0.0022	0.0010	-55%
	0.0061*	0.0031*	-49%*
	0.0027	0.0031	15%
400mm, Scaled amplitude *	0.0054	0.0054	0%
	0.0022	0.0018	18%
	0.0061*	0.0053*	-13%*
	0.0027	0.0053	96%
440mm	0.0086	0.0056	-35%
	0.0041	0.0018	-56%
	0.0049	0.0035	-29%
440mm, Scaled amplitude	0.0086	0.0086	0%
	0.0041	0.0027	-34%
	0.0049	0.0054	10%
480mm	0.0220	0.0092	-58%
	0.0068	0.0033	-51%
	0.0026	0.0028	8%
480mm Scaled amplitude	0.0220	0.0220	0%
	0.0068	0.0079	16%
	0.0026	0.0067	158%

Table 7: Comparison of lab and simulation peaks(Magnitude)

\*Uncertain lab result, further elaborated in Chap.7.3

In order to test the linearity to see that we, in fact, are below the strain rates resulting in hyperelastic nonlinear behavior, the simulation was run with a static deflection analysis with the forces: 0.1N, 1N, and 10N, the results showed an absolute linear relation to the force input.

Force (N)	Displacement (mm)
0.1	1.5e-4
1	1.5e-3
10	1.5e-2

Table 8: Testing the linear relationship between force and displacement when using Neo-Hookean hyperelastic material model



---

## 7 Discussion

Managing to set up a full 3D simulation of a vibration-damped tool holder with a high focus on applying a material model to accurately describe the rubber behavior has been a time-consuming competence intensive task. Running the simulations with seemingly good results, was therefore an important milestone during the thesis work. Performing lab experiments at Sandvik Teeneess enabled parameter tuning of the rubber material model, resulting in very satisfactory results in terms of peak frequency values, although the simulation and lab results are not equal. The difference between lab and simulation may be an effect of incomplete simulation modeling, imperfect lab setup, and monitoring errors. The choices, methodology, results, roots of error, and connections between findings and literature will be discussed in this chapter along with the implications of the thesis work.

### 7.1 Simulation and Lab Setup

The modeling of the components is done in a simplified matter, both in order to replicate the necessary geometry, and to keep the company secrets of Sandvik Teeneess intact. Damper mass inner/outer diameter and length, rubber spring geometry, and boring bar outer and inner diameters are equal to the real-world components. The boring bar body has material properties confirmed by Sandvik Teeneess representant, the material damping used in the simulation for both the boring bar and rubber springs was said to be "close to reality". The simulations conducted in this thesis all use the modal frequency domain solver. As the frequency peaks in the magnitude were known from the lab experiments, it could easily be validated that the modal analysis picks up the relevant frequencies, by looking at the peaks in the simulations, in relation to the lab results. For an analysis without a real-life result for verification, a direct frequency domain solver would provide more safety for getting the frequency response(Ivar 2023), but it requires a lot more computational power which was not available for me and my thesis. The direct solver solves the whole model in one, instead of the reduction based on the eigenfrequency study as the modal analysis does. This might result in a better prediction of the magnitudes and a lower deviation between the calculated 2nd. Lamé parameter and the final tuned value due to a better implementation of the damping in the model and its responses in the frequency sweep.

When importing the simplified TMD assembly into Comsol, the assembly is formed as a union, creating an object with connected domains, separated by common boundaries with the adjoining entities. If joined as an assembly the geometry would still be joined into a single object, but with disconnected domains and mesh, the boundaries in contact have identity pairs securing continuity in the physics. "Form assembly" is useful when modeling unequal types of contact and boundary conditions between parts(Comsol 2023b). For future investigation, it would be interesting to test with different types of contact modeling to see how this affects especially the magnitude of the simulation result.

Due to the way boundary conditions are set on the simplified boring bar with TMD assembly, it becomes unnaturally stiff compared to the lab experiments. This is due to the real-world fixturing not being completely rigid like the simulation. Exactly how big the difference is between the simulation and lab setup is hard to estimate, but it would be possible to model a fixed boundary condition with a given stiffness locking the boring bar body resembling the lab setup. It is possible that the peaks in the range: 700 Hz - 1100 Hz come from vibrations in the fixturing of the tool in the CNC lathe.

Looking at the lab magnitude plot of the boring bar with TMD at 400mm free length Fig.26. The peak at 284Hz is rough around the edges, this might indicate noise in the measurements, and if compared to the trend in the 440mm free end and 480mm free end, the peak seems unnaturally high Fig.24. Another element is that there are three peaks instead of two peaks that have been the case for the 440mm and 480mm free length. If we take a look at the trend for the two peaks of the curves in the range: 200 Hz - 300 Hz it seems like the left peak increases in magnitude with increased free length, and the opposite happens with the right peak with increased free length. It also looks like the peaks become closer to each other with increased free length. Even though we

---

performed three different free-length experiments, it is hard to draw any sound conclusion from the data, and in retrospect, a greater number of free-length variations would be beneficial for looking at trends in the curve with changes in free length.

## 7.2 Parameter Tuning

As mentioned in the methodology chapter, the TMD translation case was used as the basis for the parameter tuning of the hyperelastic Neo-Hookean material model for the rubber springs.

When tuning the rubber material parameters, the 2nd. Lamé parameter was found effective to tune the frequency of the peaks in the frequency response simulations. The final tuned parameter value deviated surprisingly much from the initially calculated 2nd. Lamé parameter. Starting at the initially calculated value: 2.568 Mpa giving 144 Hz, towards the target peak value found in the lab of 122 Hz, resulting in a final value of 1.75 MPa and a frequency: 119 Hz. Deviation:  $2.568 \text{ Mpa} - 1.75 \text{ Mpa} = 0.818 \text{ Mpa}$ , or 32% lower than calculated. The reason for this may be due to an incorrect contact modeling, or due to the modal solver, but this has to be tested in future research.

The Isotropic structural loss factor was used to adjust the width and height of the curve in the simplified TMD translation simulation. Landing on 0.08 gave satisfactory results based on a visual inspection of the curve. Visual verification was seen as good enough, as opposed to a more analytic or numerical tuning method, due to the frequency fitting of the peaks being set as a high priority, and the magnitude having a lower priority. Looking at the TMD translation and rotation plots Fig.22, the magnitude curves become distant from each other at the second peak(rotation): 244Hz(lab). Why the relative deviation is larger at the rotation mode is unclear. Part of the reason can be that the accelerometer might not have been placed all the way to the edge of the damper mass, which only would affect the rotation mode magnitude. But the simulation contact modeling between the damper mass and the rubber elements formed as a union in Comsol, might also not limit movement correctly. In real life, the TMD assembly has some degree of axial pressure due to a hollow axle(center tube) used to hold the components tight in place and used to tune the damper. This hollow axle and the tension introduced by it might restrain the deflection of the damper mass to some degree as well as compress the rubber spring disc, which would give a lower calculated initial value for the 2nd. Lamé parameter due to the change in thickness.

## 7.3 Interpretation of Simulation and Lab Results

Taking the peaks of the lab and simulation frequency response curves into consideration. The frequency and magnitude values of the peaks have been seen as a good way of quantifying the simulation capabilities of predicting real-world dynamics. The peak values are of high interest when it comes to tuning and identifying frequency ranges exposed to resonance.

The peaks are identified by my self-made Python script handling both simulation and lab data and plotting them with frequency and magnitude values. The values were then filled into tables and the error of the simulated values are calculated. For the TMD cases, the translation and rotation case is the only one used, as both frequency and magnitude of the first mode is very similar to the pure translation case and therefore deemed excessive. For the magnitude overview, both original and magnitude-adjusted values are used to give insight into how the error changes after adjusting.

Looking at the frequency overview in Table 6 We can clearly see that the simulation is highly capable of predicting the peak frequencies of the real-world system after parameter tuning with the TMD translation case. With errors ranging from -3% to 8%, the error width is 11%. But if we exclude the 8% peak, discussed as a possible subject of measurement noise the range is only from -3% to 0% giving 3% width, which is considered a huge success taking in the objective of max 5% error. All errors except for the 8% error at the 400mm case are on the negative error side and therefore the 2nd. Lamé parameter could possibly be increased slightly to decrease the max absolute error. This conforms with the fact that the simulation peak in the TMD translation case was at 119Hz after the tuning was finished and the lab magnitude peak was at 122 Hz. But the error in the case of finished tuning was only 2% and this was seen as good enough. As a

---

former CNC operator, I was taught a golden rule for manufacturing, based on productivity and predetermined tolerances: "as coarse as possible, and as accurate as required". So when I reached an error within my objective, I was satisfied. Not knowing if the trend would become a negative error due to the negative error in the tuning case was also a reason to not spend more time reaching 0% error. The mean of the absolute error values is 1%, indicating a highly successful ability of the simulation to predict real-life behavior.

Magnitude deviation was expected from the start of the thesis and set as a secondary priority to accurate simulation of the frequencies. The magnitude overview in Table 7 confirms what we could see in the plots, that the magnitude has a significantly larger error than the frequencies. But even though the errors are larger, it is not seen as a failure. Plotting the curves, the overall curve shape as well as the width and height ratio of the peaks are well suited for magnitude adjustment, providing very good agreement between lab and simulation from the first peak up to the area of the second peak. As the error varies within the cases with few clear patterns, it is likely that the problem with the model is not of linear nature. Taking the mean of the absolute errors in the original simulations results in: 73% error, while the mean of the absolute errors of the scaled simulation magnitude gives: 60% error. This indicates some improvement in scaled simulation magnitude. Scaling based on the first peak values of the lab and simulation was done to create a clearer picture of how the magnitude curves follow each other up to and beyond the first peak as this is also the largest frequency span without other peaks. Other ways of scaling may create a lower overall error and a better agreement of the curves all over and would be a point for further research. A pattern that is possible to see from the unscaled free-length plots is that the simulation magnitude of the first and second peaks is consistently below the lab results. This is in opposition to the TMD cases where the simulation magnitude is above the lab magnitude for both cases and both peaks in the TMD translation and rotation case. This can occur from the Rayleigh damping parameters in the boring bar not being absolutely accurate.

## 7.4 Goals and objectives

The eigenfrequency deviation is within the objective for the thesis of a maximum value:5% as seen in Table 6 with the exception of the 400mm free length of 8%. Variations in the amplitude error for each case are also an interesting parameter, as we would want these errors to be as similar as possible for each case, resulting in the best curve fit for the peaks with magnitude correction. The magnitude errors can be seen in Table 7

For the boring bar with TMD cases, spikes can be observed in the lab magnitude in the range of 700 Hz - 1100 Hz. Simulation outputs for the range showed no increased response. It was evaluated to be frequencies coming from a high stiffness solid component, and therefore possibly the machine structure and the tool fixturing itself.

Looking at the plot of the lab results Fig.24 the 400mm plot has a relatively high spike at 286Hz, better visualized in Fig.26. Without further knowledge of the way data is treated in Sanvik Teeneess lab software, it is hard to conclude, but based on the fact that the system becomes stiffer, we could argue that a downward trend in the peaks with decreasing free length would be normal. It has therefore been a high suspicion that the peak is unnaturally high, and may stem from measurement noise.

---

## 7.5 Addressing Research Questions

In the context of the main research question "How can a finite element model of a vibration-damped tool holder for internal turning operations be developed and validated using COMSOL Multiphysics, with a focus on accurately representing and tuning the behavior of rubber to return simulation results close to real-world behavior?". The Comsol simulation, with its rubber model and contact definitions, performs very well in terms of peak frequency behavior. However, it lacks the same accuracy when it comes to the magnitude. To improve the performance of the simulations, more focus should be put on accurately describing the contact at the rubber spring boundaries and the effect of axial pressure holding the TMD assembly together. Research needs to be done towards a direct solver being used on the simulations, but this requires high computational capacity.

"How do the results of the finite element simulations and experimental validation conform with each other, and which parameters are best used to tune the rubber constitutive model?\*" The validation of the hyperelastic material model is primarily based on comparing the simulation results with the experimental data. If these plots match closely in their behavior, then it's a strong indicator that the chosen material model is an accurate representation of the material's real behavior. But many other factors in the simulation setup come into play, like contact modeling, meshing, and more, which can be hard to distinguish in the result.

Choosing the hyperelastic material model is justified based on the assumption of the rubbery phase of the material and the validation from the stationary study showing a linear relationship between load and deformation within the deformation ranges found in the output of the frequency domain studies in Table 8. The Neo-Hookean model was chosen due to its simplicity and low number of parameters that needed to be tuned.

"What are the key material properties and constitutive models of rubber that need to be considered for accurately modeling their behavior in a vibration-damped tool holder?", it has been found that the choice of a hyperelastic material model over a viscoelastic model was appropriate to describe the eigenfrequencies of the system. This decision was made based on the assumption that the rubber material operates within its rubbery phase temperature range Fig.9, demonstrating hyperelastic behavior. Hyperelastic materials can undergo large deformations and then return to their original shape once the load is removed.

However, there might be a presence of viscoelastic behavior in the real application that isn't captured in the simulations by the hyperelastic Neo-Hookean material model. Viscoelastic materials exhibit both elastic and viscous behavior, meaning they deform over time when subjected to a constant strain, which isn't a characteristic captured by the hyperelastic model. This may affect the amplitude and contribute to the differences between lab and simulation amplitude.

The two key parameters in the hyperelastic Neo-Hookean material model, the 2nd Lamé parameter, and the isotropic structural loss factor both influence the system's frequency and amplitude responses, but in different ways.

The 2nd Lamé parameter, often denoted as the shear modulus  $G$ , determines the material's resistance to shape changes when a force is applied. An increase in this parameter results in a stiffer system that has higher eigenfrequencies and lowers the amplitude of the response. Changes in this parameter have a significant impact on both frequency and magnitude, meaning that this parameter can be finely tuned to match the system's physical properties.

The isotropic structural loss factor determines how much energy is dissipated as heat in the material during deformation. A higher value of this factor smooths the response curves, reducing the rate of change in displacement and lowering the amplitude of the response. Changes in the isotropic structural loss factor have a solid effect on the rate of change in displacement and in magnitude.

"How can the finite element model of the vibration-damped tool holder be optimized to improve its accuracy and computational efficiency, considering the complexities of the materials involved?" Further optimization for computational speed could potentially be achieved by reducing the model to beam physics, the computational speed achieved with the modal solver is already quite satisfactory.

---

Instead of focusing on further computational efficiency optimizations, future research should explore different modeling techniques for physical phenomena such as boundary contact, with the aim of increasing the simulation's approximation of the real world. This can include the use of different solver settings that are more appropriate for the specific physical problem. Further research into the rubber material used in the damper could also be of interest to better model its physical properties. If heavy computational power is available, the direct frequency domain solver should also be run as this takes in the complex value of the eigenfrequencies of the damped structures. But this solver requires data power I was not in possession of throughout my thesis.

Finally, in terms of the last research question "What experimental methodologies and techniques can be employed to validate the simulation results obtained from the COMSOL Multiphysics model, ensuring the reliability and accuracy of the findings?" Throughout the thesis, the emphasis when developing the simulations and tuning the rubber material model has been towards the eigenfrequencies. The methodology applied has been to tune the parameters based on the TMD experiments, and then keep the same parameters for the full assembly simulations of the boring bar with TMD. The method is robust in the way that it limits the number of uncertainties when tuning the rubber, but in retrospect, impulse response tests should be performed on the steel boring bar as well to ensure accurate modeling of its material damping properties. With increased data power and more time, parameter tuning(which requires many simulation runs to perform) with the direct frequency domain solver in Comsol would be of high interest to see if this fixes some of the amplitude errors in the simulation.

## 7.6 Implications of the results and my contribution

As a manufacturer of vibration-damped tool holders, it is of high priority to understand and be able to efficiently model different variations of possible design variations, pushing to make better and more efficient products. The use of powerful simulation software can enable a highly efficient development phase and reduce the number of physical prototypes needed to be made on the way to a finished product. Comsol has through this thesis proven to be an efficient tool for simulating complex structures of different materials. Furthermore, Comsol shows promising behavior towards making more accurate simulations and incorporating viscous damping in the model to fully replicate a vibration-damped tool holder. Although the technology of vibration-damped tool holders has been around for many years, the importance of economic efficiency as well as designing for a more automated production line are factors that may require a redesign of existing products. Having the possibility to perform simulations, and accurately describe real-world events allows for swift adjustments to meet market needs, and the ability to provide short lead time on special builds, research, and development of new products. A robust simulation setup and understanding of key features in the solver settings and boundary conditions can provide:

- Cost-effective validation of a wide range of concepts
- Help optimize the design for a more atomized production, assembly, and tuning of the TMDs
- Short time from idea to validation of the concept.
- Less demanding in terms of the number of people needed to perform analysis and validation than with physical production to test every concept.

Thru my autumn semester thesis and master's thesis, I have developed my simulations with a high degree of independence. Starting with no theoretical knowledge in the field of vibrations, and very limited knowledge in the Comsol software it has been a knowledge trip. The biggest challenge has without a doubt been to manage setting up the simulations in Comsol and to get useful results from the simulations. Neither I nor my advisor had any knowledge of how to perform vibration analysis in Comsol, it was therefore a great deal of help when a representant from Comsol was able to dig up some relevant theory for me to help guide the way, (Comsol 2023f) and (Comsol 2023a). The simulations have been developed by myself with no assistance in the simulation setup, I have also done all validation of the simulations independently, but with a discussion of my theory with advisor

---

Knut Sørby. Being relatively fresh in the field of vibration and damping, having such a competent advisor in these fields as well as in the fields of measurement technique has been of high importance to me throughout the thesis. For further work, it is important to recognize the short amount of time and independence, especially in the development of the simulations. Therefore, I would strongly recommend a walk thru of the simulations and validations with a senior engineer having solid knowledge in FEM simulations, preferably Comsol, and vibration theory. Throughout my thesis, I did not manage to arrange such a review, as the Comsol office in Trondheim, unfortunately, was out of capacity to help in such a short time. All though the thesis isn't reviewed by anyone with such competence, the results and margins of errors in the peak magnitudes indicate a successful simulation with surprisingly low errors on the magnitude, and a very good ability to predict the frequency of magnitude peaks measured at Sandvik Teeneess. This makes the thesis a solid foundation for further development of the Comsol simulations, incorporating fluid dynamics into the simulation models for a full-scale simulation of a real-world vibration-damped tool holder.

---

## 8 Conclusion

The research throughout the thesis has been of a high degree of independence, providing simulation results on cases similar to lab experiments performed at the Sandvik Teeness lab by Dan Östling. The data from the lab and simulation of several equal cases make the results robust and fit for evaluation. Using a low-level assembly (TMD without oil) ensured as few unknown elements and disturbances as possible when tuning the unknown rubber material parameters to ensure accurate simulations. Comparing simulations with tuned rubber material parameters to lab results showed promising margins of errors, leading to believe that Comsol is a powerful tool for commercial use in the production of vibration-damped tool holders.

### 8.1 Summary of Key Findings

Using the case: TMD Translational Ref:19a, as a tuning basis resulted in the consistent prediction of peak frequencies for all cases. The resulting parameter values after tuning:

- 2nd. Lamé parameter ( $\mu$ ) : 1.75Mpa
- Isotropic loss factor: 0.08

The value of the 2nd. Lamé parameter ended 32% lower than the value calculated from the lab data. The reason for the deviation is unknown but is likely affected by: Unnaturally stiff simulation setup, incomplete modeling of the axial compression in the TMD assembly, the use of a modal solver over a direct solver in Comsol, and incomplete contact modeling. When tuning the rubber material isotropic loss factor I wanted to stay close to the value of 0.06 as Sandvik indicated this value as close to reality. Ending at 0.08 gave very good magnitude agreement in the tuning case after adjustment Fig.21. After fully tuning the rubber material parameters, results showed very good performance in the estimation of eigenfrequencies with less than 4% error, but the performance in predicting the magnitude, although better after correction, should be subject to improvement to make the simulations useful in the commercial segment. Magnitude deviations of the degree seen in the results are accepted in this thesis, as it was a lesser priority compared to frequency accuracy. It is necessary to continue research and development to develop a simulation model including viscoelastic damping, to reach a point where the simulations ultimately can streamline the product development phase.

### 8.2 Further Work

The thesis concludes with a solid foundation for further work and development, deeming Comsol Multiphysics as a highly competent simulation tool to simulate vibration-damped tool holders. competent personnel should review the thesis work to do a professional evaluation on the continuation of the project towards commercial use.

In the event of continuation, the following points are seen as important areas of further work:

- Using the direct frequency domain solver in Comsol to run the simulations instead of the modal solver. New parameter tuning might be necessary, and high computational power is easily accessible for most engineering companies.
- Investigating different ways of modeling contact in Comsol. With the rubber-steel-rubber boundaries as subject to the contact modeling.
- Include some degree of flexibility in the boring bar fixture in the simulation to account for the flexibility in the real-world lab experiments and the machine structure flexibility.
- Perform an impulse test on the boring bar to find the solid damping in the boring bar body.

- 
- Perform more impulse tests on a boring bar with TMD to make detection of magnitude and peak trends with varying free length.
  - Include viscous damping in the simulation model after improving the magnitude performance and the roots of error in the 2nd. Lamé parameter.
  - Do further research on the TMD assembly and understand the forces at play in a steady state of the TMD.



---

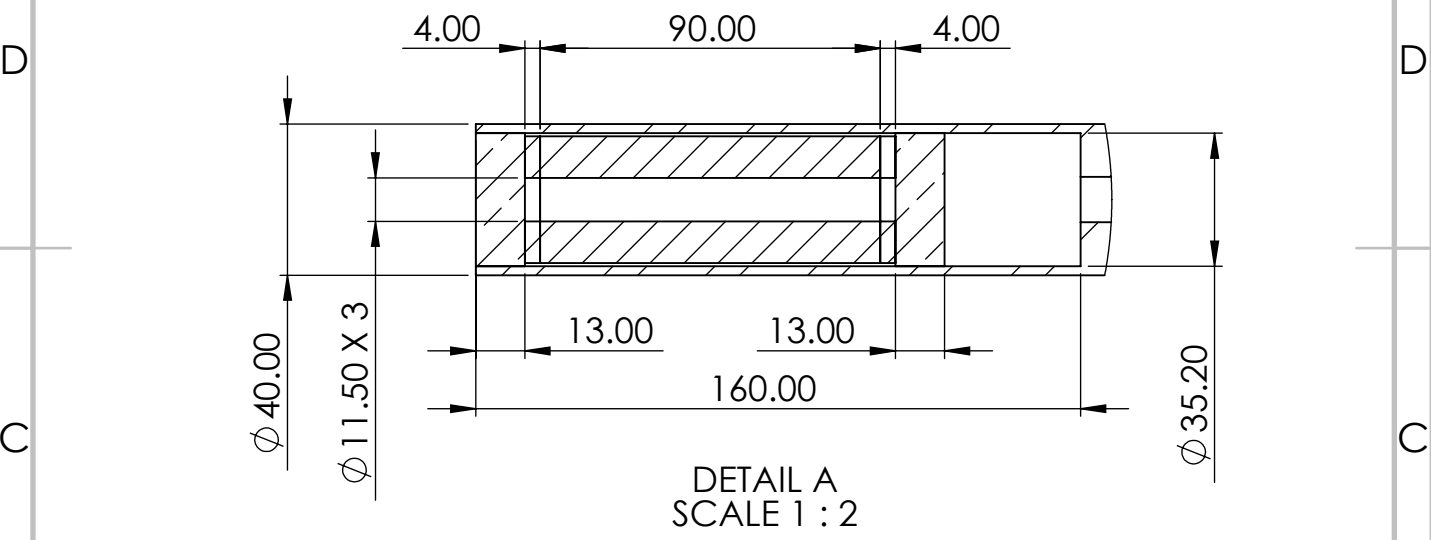
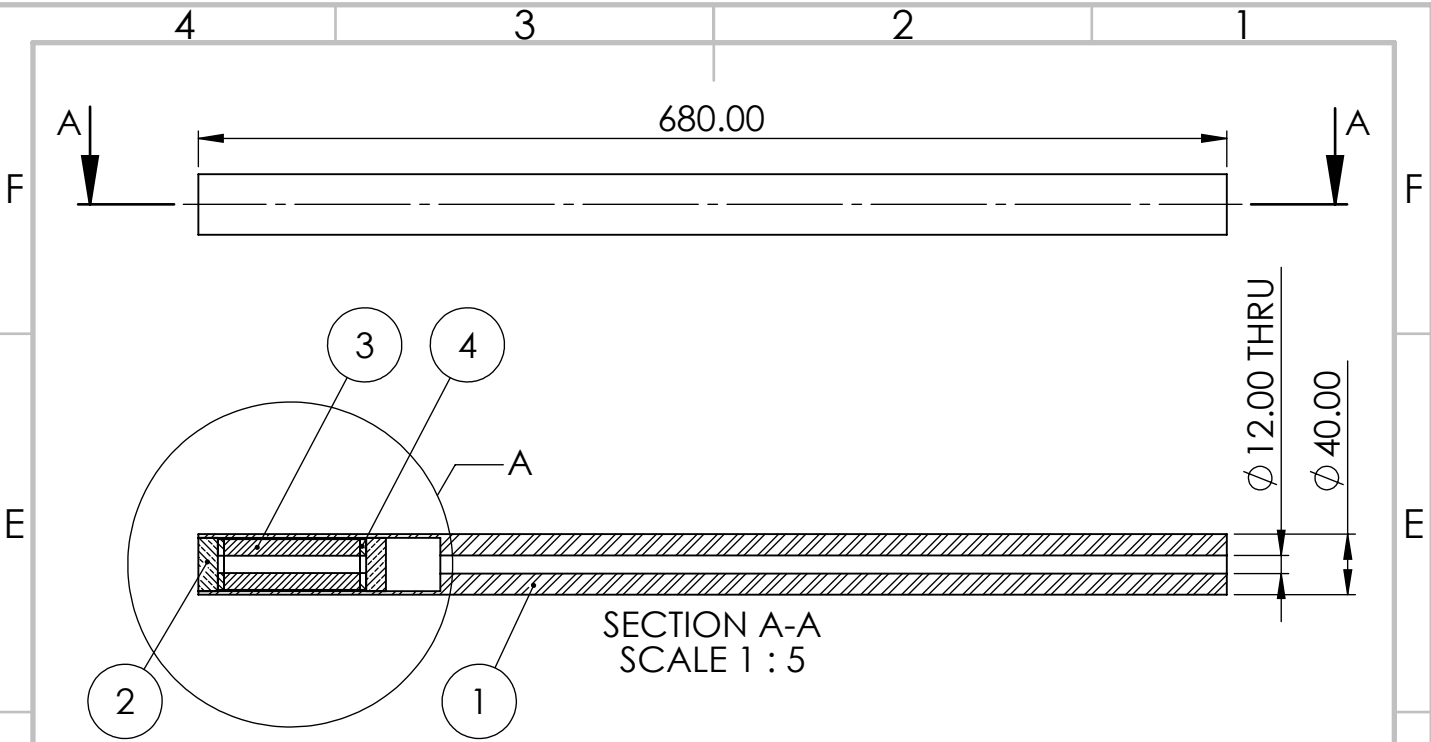
## Bibliography

- Altintas, Yusuf (2012). *Manufacturing Automation: Metal Cutting Mechanics, Machine Tool Vibrations, and CNC Design: Second Edition 978-1-107-00148-0* -.
- Asana (2023). *How to Write An effective Project Objective*. Asana. URL: <https://asana.com/resources/how-project-objectives> (visited on 28/03/2023).
- Branesh, Ajin et al. (10th June 2020). *Vibrational Analysis Over An Aircraft Wing Section*. DOI: 10.13140/RG.2.2.10410.85449.
- Cheng, Alexander H. -D. and Daisy T. Cheng (1st Mar. 2005). ‘Heritage and early history of the boundary element method’. In: *Engineering Analysis with Boundary Elements* 29.3, pp. 268–302. ISSN: 0955-7997. DOI: 10.1016/j.enganabound.2004.12.001. URL: <https://www.sciencedirect.com/science/article/pii/S0955799705000020> (visited on 25/05/2023).
- Comsol (2017). *Detailed Explanation of the Finite Element Method (FEM)*. URL: <https://www.comsol.com/multiphysics/finite-element-method?parent=physics-pdes-numerical-042-62> (visited on 24/05/2023).
- (2023a). *Eigenfrequency Analysis*. URL: <https://www.comsol.com/multiphysics/eigenfrequency-analysis?parent=structural-mechanics-0182-212> (visited on 24/05/2023).
  - (2023b). *Form Union and Form Assembly*. COMSOL. URL: <https://www.comsol.com/video-training/getting-started/form-union-form-assembly-geometry-finalization-methods> (visited on 07/06/2023).
  - (2023c). *Frequency Domain, Modal*. URL: [https://doc.comsol.com/5.5/doc/com.comsol.help.comsol/comsol\\_ref\\_solver.27.026.html](https://doc.comsol.com/5.5/doc/com.comsol.help.comsol/comsol_ref_solver.27.026.html) (visited on 08/06/2023).
  - (2023d). *Loss Factor Damping*. URL: [https://doc.comsol.com/5.5/doc/com.comsol.help.sme/sme\\_ug\\_modeling.05.084.html](https://doc.comsol.com/5.5/doc/com.comsol.help.sme/sme_ug_modeling.05.084.html) (visited on 31/05/2023).
  - (2023e). *Optimize Your Multiphysics Models with the Optimization Module*. COMSOL. URL: <https://www.comsol.com/optimization-module> (visited on 29/05/2023).
  - (2023f). *Vibration Analysis of a Deep Beam*. COMSOL. URL: <https://www.comsol.com/model/vibration-analysis-of-a-deep-beam-20301> (visited on 08/06/2023).
  - (2023g). *What Is Structural Mechanics? - An Introductory Guide*. URL: <https://www.comsol.com/multiphysics/introduction-to-structural-mechanics> (visited on 24/05/2023).
- Den Hartog, J. P. (1947). *Mechanical Vibrations*. Massachusetts institute of technology.
- Harish, Ajay (5th Aug. 2016). *Modeling Elastomers Using FEM: Do’s and Dont’s — SimScale Blog*. SimScale. URL: <https://www.simscale.com/blog/tips-modeling-elastomers-using-fem/> (visited on 19/05/2023).
- Ivar, Kjelberg (2023). *The frequency domain study vs. the frequency domain modal study*. URL: <https://www.comsol.com/forum/thread/28551/The-frequency-domain-study-vs-the-frequency-domain-modal-study-> (visited on 07/06/2023).
- Kraus, Michael A. et al. (1st Oct. 2017). ‘Parameter identification methods for visco- and hyperelastic material models’. In: *Glass Structures & Engineering* 2.2, pp. 147–167. ISSN: 2363-5150. DOI: 10.1007/s40940-017-0042-9. URL: <https://doi.org/10.1007/s40940-017-0042-9> (visited on 20/05/2023).
- Objectives and goals: SMART* (2023). Objectives and goals: Writing meaningful goals and SMART objectives - MN Dept. of Health. URL: <https://www.health.state.mn.us/communities/practice/resources/phqtoolbox/objectives.html> (visited on 28/03/2023).
- Ph.D, Lukasz Skotny (24th Jan. 2019). *What are Nodes and Elements in Finite Element Analysis?* Enterfea. URL: <https://enterfea.com/what-are-nodes-and-elements-in-finite-element-analysis/> (visited on 25/05/2023).
- Practical Engineering (28th Aug. 2018). *Why the Tacoma Narrows Bridge Collapsed*. URL: <https://www.youtube.com/watch?v=mXTSnZgrfxM> (visited on 25/05/2023).
- Schmitz, Tony L. and K. Scott Smith (2019). ‘Modal Analysis’. In: *Machining Dynamics: Frequency Response to Improved Productivity*. Ed. by Tony L. Schmitz and K. Scott Smith. Cham: Springer International Publishing, pp. 7–66. ISBN: 978-3-319-93707-6. DOI: 10.1007/978-3-319-93707-6.2. URL: <https://doi.org/10.1007/978-3-319-93707-6.2> (visited on 25/05/2023).
- Sims, Neil D. (3rd Apr. 2007). ‘Vibration absorbers for chatter suppression: A new analytical tuning methodology’. In: *Journal of Sound and Vibration* 301.3, pp. 592–607. ISSN: 0022-460X. DOI: 10.1016/j.jsv.2006.10.020. URL: <https://www.sciencedirect.com/science/article/pii/S0022460X06007930> (visited on 08/06/2023).

- 
- Sørby, Knut (30th Jan. 2016). ‘Development and Optimization of Vibration-Damped Tool Holders for High Length-to-Diameter Boring Operations’. In: *High Speed Machining 2*. DOI: 10.1515/hsm-2016-0005.
- Venkateshan, S. P. and Prasanna Swaminathan (1st Jan. 2014). ‘Chapter 13 - Laplace and Poisson Equations’. In: *Computational Methods in Engineering*. Ed. by S. P. Venkateshan and Prasanna Swaminathan. Boston: Academic Press, pp. 529–573. ISBN: 978-0-12-416702-5. DOI: 10.1016/B978-0-12-416702-5.50013-2. URL: <https://www.sciencedirect.com/science/article/pii/B9780124167025500132> (visited on 25/05/2023).
- What is Hooke’s Law?* (2023). *What is Hooke’s Law? (article)*. Khan Academy. URL: <https://www.khanacademy.org/science/physics/work-and-energy/hookes-law/a/what-is-hookes-law> (visited on 12/04/2023).

---

## Appendix



ITEM NO.	PART NAME	DESCRIPTION	QTY.
1	Boring Bar		1
2	TMD Restrainer		2
3	TMD Damper Mass (OD:33.5mm)		1
4	TMD Rubber Spring (OD:33.5mm)		2

UNLESS OTHERWISE SPECIFIED:  
 DIMENSIONS ARE IN MILLIMETERS  
 SURFACE FINISH:  
 TOLERANCES:  
 LINEAR:  
 ANGULAR:

FINISH:

DEBURR AND  
 BREAK SHARP  
 EDGES

DO NOT SCALE DRAWING

REVISION

	NAME	SIGNATURE	DATE
DRAWN			
CHK'D			
APPV'D			
MFG			
Q.A			

TITLE:  
**Bom with damper**<sup>A4</sup>  
 DWG NO.  
 SCALE:1:10  
 SHEET 1 OF 1

